



The Gateway Cities Air Quality Action Plan

TASK 2B3 DATA ANALYSIS TO ASSESS THE REPRESENTATIVES OF MODELED NEAR-ROADWAY CONCENTRATIONS

Final

September 2011

PREPARED FOR:

Los Angeles County Metropolitan Transportation Authority
Gateway Cities Council of Governments (GCCOG)

PREPARED BY:

ICF International
1 Ada, Suite 100
Irvine, CA 92618
Contact: Edward Carr
(949) 333-6600

Contents

| | | |
|-------------|---|----|
| 1. | Introduction | 1 |
| 2. | Review of Available Monitoring Data | 2 |
| 2.1 | SCAQMD Monitoring Data | 2 |
| 2.2 | Other Monitoring Studies | 2 |
| 3. | Review of Available Modeling Data | 4 |
| 3.1 | Additional Dispersion Modeling | 4 |
| 4. | Model-to-Monitor Comparison of Near-Roadway Concentrations | 6 |
| 4.1 | Comparison of Hourly Concentrations | 6 |
| 4.2 | Model-to-Monitor Comparison of Spatial Gradients..... | 8 |
| 4.3 | Sensitivity Analysis | 9 |
| 5. | Discussion and Recommendations | 11 |
| 6. | References | 54 |
| Appendix A. | Comparative Studies | |

Figures

| Figure | Page |
|--------|--|
| 1 | Locations of the Air Quality (East, West, and Del Amo) and Meteorological Monitoring Station (Long Beach) from the SCAQMD Dataset..... 14 |
| 2 | Two Locations of the Air Quality (Monitor 1 and 2) and SCAQMD Meteorological Monitoring Station (Compton) from the Ning et al. (2010) 15 |
| 3 | Scatter Plot of Model-Predicted and Monitored CO Concentrations..... 15 |
| 4 | Scatter Plot of Model-Predicted and Monitored NO _x Concentrations 17 |
| 5 | Scatter Plot of Model-Predicted and Monitored CO Concentration for Intra-Day Periods during Summer 18 |
| 6 | Scatter Plot of Model-Predicted and Monitored CO Concentrations for Intra-Day Periods during Winter..... 19 |
| 7 | Scatter Plot of Model-Predicted and Monitored NO _x Concentrations for Intra-Day Periods during Summer 20 |
| 8 | Scatter Plots of Model-Predicted and Monitored NO _x Concentrations for Intra-Day Periods during Winter..... 21 |
| 9 | Q-Q Plot between Model-Predicted and Monitored Concentrations (PPB) during Summer 23 |
| 10 | Q-Q Plot between Model-Predicted and Monitored Hourly Concentrations (PPB) during Winter 24 |
| 11 | Comparison of Model-Predicted and Monitored Concentration Distributions (PPB) for Model Predictions, Based on 75 Receptors in the Vicinity of Monitoring Location 25 |
| 12 | Comparison of Predicted Concentrations by CAL3QHC and Monitored CO Concentrations at Three at Elizabeth, NJ., and St. Paul MN., in a NCHRP Study 26 |
| 13 | Scatter Plots of Dilution Ratios Calculated from Model Predictions and Monitored Concentrations 40 |
| 14 | Scatter Plots of Dilution Ratios Calculated from Model-Predicted and Monitored CO Concentration Data for Four Intra-Day Periods during Summer..... 41 |
| 15 | Scatter Plots of Dilution Ratios Calculated from Model-Predicted and Monitored NO _x Concentration Data for Four intra-Day Periods during Summer..... 42 |

| | | |
|----|---|----|
| 16 | Scatter Plots of Dilution Ratios Calculated from Model-Predicted and Monitored CO Concentration Data for Four Intra-Day Periods during Winter | 43 |
| 17 | Scatter Plots of Dilution Ratios Calculated from Model-Predicted and Monitored NOx Concentration Data for Four Intra-Day Periods during Winter | 44 |
| 18 | Temporal Profiles of Light-Duty (Passenger 2/3-Axle Trucks) and Heavy-Duty (4 or More Axle Vehicles) Traffic on the I-710 from Historical (15 May–15 September 2002) Caltrans Weigh-In Motion Sensors. | 48 |
| 19 | Scatter Plots of Observed and Modeled NOX Concentrations at the East Monitor Using the Temporal Profile Used in I-710 EIR/EIS (Dots in Blue, Left Panels) and the Profile from Caltrans I-710 Weigh in Motion Traffic Volume Data (Dots in Red, Rig | 49 |
| 20 | Scatter Plots of Observed and Modeled NOX Concentrations at the East Monitor Using the Temporal Profile Used in I-710 EIR/EIS (Dots in Blue, Left Panels) and the Profile from Caltrans I-710 Weigh In Motion Traffic Volume Data (Dots in Red, Rig | 50 |
| 21 | Scatter Plots of Observed and Modeled NOX Concentrations at the East Monitor Using the Temporal Profile Used in I-710 EIR/EIS (Dots in Blue, Left Panels) and the Profile from Caltrans I-710 Weigh In Motion Traffic Volume Data (Dots in Red, Rig | 51 |
| 22 | Scatter Plots of Observed and Modeled NOX Concentrations at the East Monitor Using the Temporal Profile Used in I-710 EIR/EIS (Dots in Blue, Left Panels) and the Profile from Caltrans I-710 Weigh In Motion Traffic Volume Data (Dots in Red, Rig | 52 |
| 23 | Scatter Plots of Observed and Modeled NOX Concentrations at the East Monitor Using the Temporal Profile Used in I-710 EIR/EIS (Dots in Blue, Left Panels) and the Profile from Caltrans I-710 Weigh In Motion Traffic Volume Data (Dots in Red, Rig | 53 |

Tables

| Table | Page |
|--|------|
| 1 Pearson Correlation Coefficients between Model-Predicted and Monitored Concentrations Hourly Concentrations | 22 |
| 2 Pearson Correlation Coefficients between Model-Predicted and Monitored Hourly Concentrations Using the | 22 |
| 3 Comparison of Average, Median, 10th Percentile, and 90th Percentile of Model-Predicted and Monitored CO Concentrations (PPB) | 27 |
| 4 Comparison of Average, Median, 10th Percentile and 90th Percentile of Model-Predicted and Monitored NOx Concentrations (PPB)..... | 28 |
| 5 Statistical Comparison of Model-Predicted and Monitored Hourly CO Concentrations (PPB) | 29 |
| 6 Statistical Comparison of Model-Predicted and Monitored Hourly NOx Concentrations (PPB) | 30 |
| 7 Distribution of the Ratio of Model-Predicted to Monitored CO Concentrations (PPB) | 31 |
| 8 Distribution of the Ratio of Model-Predicted to Monitored NOx Concentrations (PPB) | 32 |
| 9 Comparison of Average, Median, 10th Percentile, and 90th Percentile of Best Model-Predicted CO Concentrations at Receptors Parallel to the Roadway and Monitored CO Concentrations (PPB) | 33 |
| 10 Comparison of Average, Median, 10th Percentile and 90th Percentile of Best Model-Predicted NOx Concentration at Receptors Parallel to the Roadway and Monitored NOx Concentrations (PPB)..... | 34 |
| 11 Statistical Comparison of Best Model-Predicted CO Concentration at Receptors Parallel to the Roadway and Monitored CO Concentrations (PPB)..... | 36 |
| 12 Statistical Comparison of Best Model-Predicted NOx Concentration at Receptors Parallel to the Roadway and Monitored NOx Concentrations (PPB)..... | 37 |
| 13 Distribution of the Ratio of Best Model-Predicted CO Concentration at Receptors Parallel to the Roadway and Monitored CO Concentrations | 38 |
| 14 Distribution of The ratio of Best Model-Predicted NOx Concentration at Receptors Parallel to the Roadway and Monitored NOx Concentrations | 39 |

| | | |
|----|---|----|
| 15 | Comparison of the Average, Median, 75th and 90th Percentile of Modeled and Monitored Dilution Ratios of CO Concentrations..... | 45 |
| 16 | Comparison of the Average, Median, 75th and 90th Percentile of Modeled and Monitored Dilution Ratios of NOx Concentrations..... | 46 |
| 17 | Distribution of the Ratio of Modeled CO Dilution Ratio to Monitored CO Dilution Ratio | 47 |
| 18 | Distribution of the Ratio of Modeled NOx Dilution Ratio to Monitored NOx Dilution Ratio | 47 |
| 19 | Comparison of Monitored and Modeled CO Concentrations (PPB) for Locations with and Without the Sound Wall Using Ning et al. (2010) Data | 48 |

1. Introduction

This memo describes the comparison of the near-roadway air quality monitoring data made in close proximity to the Interstate 710 (I-710) with the corresponding modeled concentrations as modeled in the I-710 EIR/EIS. The main objective and purpose of this analysis presented in this memo is to *assess the representativeness* of the modeled near-roadway concentrations by comparing results of modeling with monitored data.¹ This model-to-monitor comparison focuses on two main features that are important to the modeling the population exposure levels and associated health risk in the near-roadway environment.

Representativeness of hourly concentrations at various distances: This component of the analysis focuses on assessing the representativeness of model-predicted hourly concentrations when compared with the near-roadway measurements collected with for similar emissions² and meteorological conditions. Because emissions and meteorological are key inputs to hourly concentrations, results are highly dependent upon the quality of these inputs.

Representativeness of spatial gradient: The concentration of pollutants due to roadway emissions is shown to decrease exponentially with downwind distance from the freeways and reach near background levels for most pollutants within 200 – 400 m (Zhu, Hinds et al. 2002; Karner, Eisinger et al. 2010). Therefore, sharp concentration gradients exist in the near-roadway vicinity, which needs to be characterized by models to reflect the potential exposure levels for determining health risk. This component of the analysis for this study herein focuses on assessing the representativeness of model-predicted spatial gradient of concentrations using the near-roadway monitored data collected with similar emissions³ and meteorological conditions.

¹ Note that this study has limitations relative to a “model performance” study where the modeled concentrations and monitored measurements are compared using statistical techniques where the monitored data are measured for the same time period and location that is modeled and on-site meteorological measurements are made as well as detailed information on vehicle activity (vehicle fleet mix, age distribution, and vehicle counts) which is estimated and then used as input to an emission factor model to determine emissions.

² Ideally vehicle activity data would have been available during the monitoring period. Given this limitation the study has adjusted the 2008 vehicle activity to represent 2009 vehicle activity by scaling the 2009 levels based on the 2008 vs. 2009 Port of Long Beach TEU numbers by month. Reduced TEU activity associated with the “Recession” were adjusted by a scaling factor adjusted by month (e.g., June 2008 vs. June 2009).

³ Ideally vehicle activity data would have been available during the monitoring period but was not collected during the study. Given this limitation the study has adjusted the 2008 vehicle activity to represent 2009 vehicle activity by scaling the 2009 levels based on the 2008 vs. 2009 Port of Long Beach TEU numbers by month. Reduced TEU activity associated with the “Recession” were adjusted by a scaling factor adjusted by month (e.g., June 2008 vs. June 2009).

2. Review of Available Monitoring Data

2.1 SCAQMD Monitoring Data

The South Coast Air Quality Management District (SCAQMD) conducted two one-month intensive monitoring campaigns at two locations in the vicinity of I-710 freeway during the winter (February–March) and summer months (July–August) of 2009. The dataset consists of two near-roadway locations at 15 m (“West” monitor) and 80 m (“East” monitor) in the prevailing downwind direction from the freeway and a prevailing upwind background site (Del Amo). Figure 1 shows the location of these monitoring sites and includes the meteorological data site used in the AERMOD air dispersion model.

During both monitoring campaigns, measurements were made of a suite of air pollutants including airborne particles (PM₁₀ and PM_{2.5}), carbon monoxide (CO), nitrogen oxides (NO_x), and air toxics compounds. These data were obtained from SCAQMD for the purposes of model-to-monitor comparison.

However, because AERMOD modeling for the I-710 Corridor Project environmental impact report/environmental impact statement (EIR/EIS) has to date only been completed for CO, NO_x, and toxicity-weighted emissions, only the CO and NO_x concentrations from both campaigns are compared in this analysis. The measurements for these two gas-phase pollutants are made at 1-hour intervals, and therefore provide a high-resolution temporal dataset for this analysis. Conclusions reached from these air pollutant findings can be extended to other gas-phase pollutants as well as for small particles.

2.2 Other Monitoring Studies

A review of recent scientific literature (peer-reviewed, conference papers and presentations) was performed to identify any recent (within the past few years) near I-710 roadway monitoring studies that could provide additional monitored data for comparison with modeled data. Appendix A contains a summary of the recent studies other than the SCAQMD I-710 study.

Kozawa et al. (2009) used a mobile platform to measure particle and gas-phase pollutants in communities close to I-710 in the summer of 2007. Although the measurements are taken at locations in close proximity to the freeways, application of this measurement data for model-to-monitor analysis would require adjustments to emissions inventory in the modeling which would introduce additional uncertainty. Furthermore, because the measurements were taken only twice during the day during the summertime, and not at the fixed monitoring sites, intra-day variation of concentrations and the model performance may not be captured. Therefore, the Kozawa et al. study is not suitable to the purposes of this analysis.

Similarly, Arhami et al. (2009) measured PM concentrations in the summer of 2007 at six sites in the communities near the Port of Los Angeles (POLA). However, because this study measured only particle concentrations, and because only one of the six study sites was in the vicinity of I-710, results of the Arhami et al. study are not suitable for the purposes of this analysis.

Moore et al. (2009) measured ultrafine particle number concentrations in 2007 at 14 monitoring sites. Although some of these sites were in the proximity of I-710, no gas-phase concentrations or particle mass concentrations were reported in this study. For this reason, the Moore et al. study is not suitable to the purposes of this analysis.

Other similar studies were found during the review that measured near-roadway concentrations. However, all of these other studies focused on measuring particle number concentrations and associated exposure to ultrafine particles in near-roadway environments.

However, based on the literature review, the data presented in a study by Ning et al. (Ning, Hudda et al. 2010) was found to be suitable for the purposes of model-to-monitor comparative analysis. This study measured the concentrations at sites within a few meters of the I-710 roadway edge and focused mainly on assessing the impact of sound walls on near-roadway concentrations. Ambient concentrations of CO and nitrogen dioxide (NO₂) were collected at two fixed monitoring sites, one along the I-710 stretch with a sound wall (Bell Gardens) and the other without a sound wall (South Gate), for 7 hours at each location during June of 2009. In addition, a mobile monitoring platform was used to measure pollutant concentrations downwind of the freeway. ICF acquired this dataset from the researchers. This dataset does not contain information on what day the data were collected, but only the time period during the day. In addition, it is strongly suspected that NO₂ concentrations are not accurate because they are significantly higher than typical near-roadway concentrations. Therefore, only CO data from the Ning et al. study was used for this analysis. Figure 2 shows the location of these monitoring sites and includes the representative SCAQMD meteorological data to be used in the AERMOD modeling.

3. Review of Available Modeling Data

The I-710 Corridor Project EIR/EIS study applied the AERMOD model to predict concentrations in the vicinity of the I-710 for the baseline year 2008, based on typical weekday 2008 traffic volumes and average speeds on the I-710. The traffic emissions are modeled as volume sources in the I-710 Corridor Project EIR/EIS. Because the modeling domain is long and encompasses an 18-mile corridor of I-710, the modeling was divided into four meteorological zones in order to use meteorological data representative of each particular zone. Concentrations of CO and NO_x pollutants were predicted for two sets of receptors in the I-710 Corridor Project EIR/EIS. The first was a regularly spaced receptor grid starting at 100 m from the I-710 out to 500 m, then every 250 m out to 2,500 m, and then every 500 m to 5,000 m. The second set includes irregularly spaced receptors placed at the sensitive sites such as schools, daycare centers, and hospitals.

3.1 Additional Dispersion Modeling

The receptors used in the I-710 Corridor Project EIR/EIS study did not include the location of the air quality measurement sites or any nearby locations. In addition, the I-710 EIR/EIS modeling was performed for the year 2008, whereas the air monitoring data was collected in 2009. Therefore, in order to compare the modeled concentrations with monitored data some adjustments were needed to make the monitored to modeled comparison. A discussion of these changes is presented in the remainder of this section.

The I-710 Corridor Project EIR/EIS used the North Long Beach meteorological station (SCAQMD station number 072) for Zone 2 modeling and the Lynwood station (SCAQMD station number 084) for Zone 3 modeling, using 2008 for both scenarios. The SCAQMD monitoring data lies within Zone 2, while the Ning et al. dataset lies within Zone 3. However, the new modeling presented in the current analysis was conducted for the year 2009. Because the Lynwood station was discontinued in late 2008, the nearby Compton station (SCAQMD Station Number 112) was used for Zone 3 modeling.

SCAQMD provided hourly temperature, relative humidity, scalar wind speed, and wind direction measurements for 2009 for the North Long Beach and Compton stations. To estimate atmospheric stability, cloud cover data from the ASOS station at Long Beach Daugherty Field (WBAN station number 23129) were used to supplement the SCAQMD North Long Beach data, and cloud cover data from the ASOS station at Hawthorne Municipal Airport (WBAN station number 03167) were used to supplement the SCAQMD Compton data. Similar cloud cover pairings were made in the I-710 Corridor Project EIR/EIS.

For both Zones 2 and 3, the air quality monitors were east of I-710. Given these monitor positions, the monitors were only concerned with analyzing hours during which the wind was blowing approximately perpendicularly across the roadway and toward the monitors. AERMOD modeling results were retained in this study only for those hours in which the wind blowing perpendicularly across the road and toward the monitors, within ± 45 degrees. For the North Long Beach data (Zone 2), hours with wind directions outside of 262 – 352 degrees were not included, leaving about 30 percent of the hours during the monitoring period between January and March hours and 51 percent of the hours between June and

August. For the Compton data (Zone 3), about 43 percent of the hours were within the wind directions between 225 and 315 degrees. For the micrometeorological surface characteristics are required by the AERMOD pre-processor program, AERMET (albedo, surface roughness, and Bowen ratio), the same analysis procedures used in the I-710 Corridor Project EIR/EIS were used in this analysis.

Briefly, these characteristics were determined from precipitation data, lookup tables from the AERMOD surface characteristic pre-processor, AERSURFACE, and the 2001 National Land Cover Database. Within a radius of 10 km from the surface meteorological station, sectors were drawn to group together similar land cover characteristics. Each month was assigned to one of 3 seasons (winter-no snow/autumn, spring, and summer). Land cover statistics were gathered within each 10-km sector, and these statistics were combined with precipitation data and lookup tables from the AERSURFACE User's Guide to calculate sector-specific, season-specific albedo and Bowen ratio values. Land cover statistics were also gathered within each sector inside a 1-km radius, and these statistics were combined with the lookup tables to calculate sector-specific, season-specific surface roughness values.

AERMET (version 11059) was run for 2009 meteorology using the above surface meteorological data, the above surface characteristics, and twice-daily upper-air meteorological data from the San Diego Miramar station (WBAN station number 03190). This produced two sets of AERMOD-ready meteorological data (one for Zone 2, one for Zone 3). The same source locations and parameters that were used in the I-710 Corridor Project EIR/EIS AERMOD modeling were used in the current analysis, with the exception of truck emissions. The majority of trucks traveling the Zone 2 and Zone 3 sections of I-710 were assumed to be related to port activity, as emissions were only available split into automobiles and trucks. Port activity, in the form of twenty-foot equivalent units, decreased in 2009 compared to 2008 by approximately 35.9 percent for the February 1 – March 11 time period, by approximately 28.7 percent for June, and by 20.7 percent for June 24 – August 19. These percent reductions were used to scale down the estimated I-710 truck emissions from 2008 to 2009 levels for these time periods.

Modeling receptors were placed at the monitor locations. AERMOD (version 11103) was run with these receptors and the above-described source parameters and meteorological data.

4. Model-to-Monitor Comparison of Near-Roadway Concentrations

4.1 Comparison of Hourly Concentrations

The comparison of model-predicted and monitored hourly concentrations of CO and NO_x is performed for locations at 15 (“West”) and 80 (“East”) m from the freeway using the SCAQMD monitoring data. In order to estimate the contribution only from the roadway emissions, the monitored concentrations are adjusted by subtracting the regional background concentrations, as measured at the Del Amo site. The analysis is performed for all hours where data is available and also separately for the following four intra-day periods: morning peak traffic hours (6–9 AM), daytime hours (10 AM–2 PM), evening peak traffic hours (3 PM–7 PM) and nighttime hours (7 PM–6 AM).

Figures 3 and 4 show the scatter plots of model-predicted and monitored hourly concentrations of CO and NO_x at all hours for winter and summer seasons. A poor correlation is observed in all the plots. The model significantly underpredicts hourly CO concentration during the winter and overpredicts hourly NO_x concentration during the summer. It can also be observed that model-predicted hourly concentration, especially for CO, lacks the temporal variation that is present in the monitored data.

Figures 5 and 6 show the scatter plots of hourly CO concentration for four intra-day periods for both seasons. The hourly CO concentration is underpredicted during almost all the intra-day periods for winter, and significantly so during the nighttime. Although large overpredictions are observed during some evening hours, the model performance during this period is somewhat better. The limited temporal variation in model concentration is due to the uniform traffic volume and speeds output from the SCAG travel demand model during each intra-day period. The evening hour during the summer and winter shows the most variation due to large change in atmospheric stability between day and night. The same pattern is seen, but to a more limited degree, in the winter period during the morning hours.

Figures 7 and 8 show corresponding plots for the hourly NO_x concentrations. In contrast to CO, hourly NO_x concentrations are overpredicted during the summer for all intra-day periods. A mixed trend is observed for winter season, with the model overpredicting during evening hours and underpredicting during the daytime and nighttime hours.

A common trend among all intra-day periods and both seasons is the limited variation in modeled concentration within the intra-day periods. This is attributed to uniform traffic volume and speeds in the South Coast Association of Governments (SCAG) travel demand model data within each intra-day period. Furthermore, the results show consistent underprediction in CO and overprediction for NO_x concentrations for both locations (i.e., 15 and 80m from the freeway) and is common across all periods (i.e., the model consistently either over- or underpredicts at both locations). Because most of the CO emissions are associated with light-duty autos this is likely attributable to an underestimation of traffic volume and/or an overestimate of average speed because CO emissions decrease with speed. Similarly, NO_x emissions are mostly associated with truck traffic and the general overprediction is likely attributable to an overestimation of truck traffic and/or an overestimate of truck speed.

Table 1 shows Pearson Correlation Coefficients between model-predicted and monitored CO and NO_x hourly concentrations for both seasons. A model that predicts monitored data perfectly would have a correlation of 1, a model that responds in an opposite direction would have a correlation of -1, and a model showing no correlation would have a value of zero. Due to the significant scatter in the data, the coefficients are close to zero. These values indicate a poor correlation between model-predicted and monitored hourly concentrations. The correlation coefficients at the 80m site (“East”) are relatively better than those at 15 m (“West”). The best correlation is only 0.515 for the morning NO_x during the winter at the 80 m site.

Meteorological inputs, especially wind direction, play an important role in determining model-predicted hourly concentrations. However, uncertainties in input often lead to significant discrepancies when model predictions are compared with monitored data. Therefore, an additional analysis was conducted that compares monitored data with model predictions at additional receptors placed within 50 m of each monitoring location, parallel to the roadway, in both directions. At each hour, the model prediction that is closest to the monitored value is determined.⁴ The Pearson Correlation Coefficients are calculated using the best predicted concentration among the parallel set of receptors. These data are presented in Table 2. Although there are small improvements in correlation coefficients using the data from receptors parallel to roadway, the magnitude of coefficients across all analysis periods still indicates poor correlation between the model predictions and monitored data. This lack of improvement provides further evidence that the underlying cause of poor model performance is the uncertainty associated with traffic activity rather than meteorology due to the limited improvement.

From an exposure perspective, the capability of the model to predict concentration distribution, especially the high-end concentrations, is most important, because health impact is associated primarily with cumulative exposure. Figures 9 and 10 show Q-Q⁵ plots for CO and NO_x concentration respectively. In addition, Tables 3 and 4 show the average, median, 10th percentile, and 90th percentile of model-predicted and monitored CO and NO_x concentrations. In general, CO has both over- and underpredictions, with a tendency to overpredict concentrations particularly at the high-end. NO_x modeled concentrations are always overpredicted by more than a factor of 2 for the highest concentrations.

Tables 5 and 6 show various metrics of bias between the model-predicted and monitored concentrations of CO and NO_x. As in the previous analysis, no major trends are observed for discrepancies between the model-predicted and monitored concentrations. Fractional bias, a measure of deviation across the period between the model prediction and monitored data, shows significant overprediction for NO_x and significant underprediction of CO during winter.

Tables 7 and 8 show the distribution of the ratios of the model-predicted to monitored CO and NO_x concentrations. The ratios greater than 1 indicate overprediction and those less than 1 indicate underprediction. The mean ratio for CO varies between 0.35 and 4.41. The median ratio of model-

⁴ The closest model-predicted value among model-predicted concentrations at parallel receptors is the one which has minimum absolute bias when compared with the observed value.

⁵ Q-Q plots are quantile-quantile plots comparing two distributions, in our case measured and observed concentrations not paired in time.

predicted to observed concentrations for most periods is less than 1.0, indicating an underprediction. The mean ratio for NO_x is consistently greater than 1.0, showing a tendency of the model to overpredict NO_x concentrations across all periods.

In some cases, the discrepancy between the model-predicted and monitored concentrations may be resolved to some extent by reducing the uncertainty in wind direction. Therefore, as discussed before, the best model-predicted hourly concentration among model predictions for a set of receptors parallel to the roadway at the monitoring locations is determined by minimizing the absolute bias. The model performance is again compared to the monitored data. The results from this comparison are shown in Tables 11 – 16. Although the data show some improvement in model performance, the magnitude of improvement is not sufficient to conclude that improving the quality of wind data would lead to significant improvement in the model performance.

4.2 Model-to-Monitor Comparison of Spatial Gradients

The analysis of spatial gradients is performed by applying the concept of *dilution ratio*. The dilution ratio is a measure of concentration gradient as a function of downwind distance. Based on the available monitoring data, the dilution ratio for the current analysis is defined as the ratio of the pollutant concentrations at 15 m and 80 m with background subtracted. Similar to the analysis to assess the hourly concentrations, dilution ratios for modeled and monitored concentrations are calculated for four intra-day periods and all hours during winter and summer seasons separately.

Figure 12 shows the scatter plots of dilution ratios calculated from the model-predicted and monitored concentration data. As with the concentration data, poor correlation is observed with both over- and underpredictions of the dilution ratio by the model. In addition, the dilution ratio calculated from model predictions is within a narrow range of 0.2 to 0.5, whereas the monitored data show a larger variation. These trends persist when dilution ratios are analyzed separately for the intra-day periods, as shown in Figures 13 to 17.

Tables 15 and 16 show the average, median, 75th, and 90th percentile of dilution ratios calculated from model-predicted and monitored concentration distributions. In general, better model performance is noted for NO_x concentrations and during the summer season. For some intra-day periods, monitored CO dilution ratios are greater than 1.0, indicating that the concentration at the 80 m location is higher than that at the 15 m location. This greater than 1.0 CO dilution ratio is attributed to the uncertainties in the measurements at both monitoring sites and at the background site, but is likely caused by monitored CO at the 80 m site having been generated from sources other than the I-710. This is most pronounced during the winter monitoring period.

Tables 17 and 18 show the distribution of the ratio of dilution ratios calculated from model-predicted and monitoring concentration data. The median ratio (50th percentile) is generally less than 1, showing that model-predicted concentrations fall more rapidly with the distance from the roadway than the monitoring data. In contrast, for summertime NO_x, the model-predicted concentration is greater than 1, showing that monitored-predicted concentrations fall more rapidly with distance from the roadway.

The model-to-monitor comparison is also performed for another dataset of near-roadway measurements. As discussed before, Ning et al. (2010) measured near-roadway concentrations of CO in the afternoon hours of summer months in the year 2009 at two fixed monitoring sites. One of these sites is along the stretch of the freeway that contains a sound wall. Because this study includes only short monitoring periods, temporal segregation of data is not feasible. Because of the limited data, a detailed statistical comparison is not meaningful. Because the monitored data were not associated with a particular day and only with the particular time during the day, average hourly concentrations were calculated for afternoon hours for both monitored and modeled data. Furthermore, regional background concentrations were not reported by Ning et al. (2010). Therefore, a typical urban regional background concentration of 1000 parts per billion (ppb) is subtracted from the measured concentrations in order to estimate the concentrations only due to the roadway emissions. Because AERMOD cannot directly model the effects of a sound wall, model runs for both locations were conducted as though no sound wall exists.

As shown in Table 19, the model generally underpredicts the CO concentration for both monitoring sites and significantly so during the mid-afternoon hours. The measured CO concentrations are consistently higher for the location without the sound wall. Although this trend is observed in modeled concentrations, it may only be attributed to changes in emissions because AERMOD did not explicitly model the presence of a physical barrier to the dispersion.

4.3 Sensitivity Analysis

The I-710 EIR/EIS modeling protocol used traffic volumes generated from the travel demand model. These volumes lacked hourly temporal variation and were segregated into the four intra-day periods, identical to those used in this analysis. Consequently, as discussed earlier, the model predictions lacked hourly temporal variation that is observed in the monitored data. To examine the importance of the hourly variation in traffic activity we conducted a sensitivity analysis using an alternative temporal profile for traffic activity.

The California Department of Transportation (Caltrans), collects weigh-in-motion data on major freeways⁶ throughout the state that can be used to determine the number and type of vehicles on an hourly basis from sensors embedded in the roadway. For the I-710 data, sensors are embedded at milepost 11.5 about ¾ mile north of the Long Beach Blvd. and I-710 interchange. Unfortunately, no data was available from Caltrans from 2008 or 2009. However, historical data from the time period May 15, 2002 through September 15, 2002 was available and was categorized by light-duty (passenger and 2/3 axle trucks) and heavy-duty (4 axles or higher) vehicle type. This profile was used to characterize the hourly change in activity while still retaining the same total emissions per day as used in the I-710 EIR/EIS modeling.

Figure 18 shows the number of vehicles per hour from this historical data for light- and heavy-duty vehicles based on the Caltrans weigh-in-motion data. As expected, there is a significant daily variation in

⁶ <http://www.dot.ca.gov/hq/traffops/trucks/datawim/>

the traffic volumes for both vehicle types. The light-duty vehicle traffic volumes show distinct morning and afternoon peaks on weekdays and only evening peak during the weekend days. The traffic volume of heavy-duty vehicles peaks during the morning hours (8 AM to noon). However, the weekend traffic volumes for heavy-duty vehicles are significantly smaller than weekday traffic volumes. Traffic volumes for both light- and heavy-duty vehicle traffic volumes on weekdays do not differ significantly from each other.

The concentration of NO_x is predicted at the 15-m (west) and 80-m (east) SCAQMD monitoring locations using this weight-in-motion temporal profile, keeping other parameters identical to the setup described in Section 3. The model-to-monitor concentrations are shown using scatter plots and report the new correlation coefficients. As before, the comparison is done separately for each combination of the four intra-day periods, two monitoring locations and two seasons. In addition, the correlations and scatter plots using this activity profile are shown side by side with those modeled using the I-710 EIR/EIS profile. These results are shown in Figures 19–23.

Applying the historical Caltrans weigh-in-motion vehicle volumes significantly improved the correlation between monitored and modeled data. The improvements are observed for all intra-day periods, at both locations, and during both summer and winter seasons. The improvement using the weigh-in-motion data is seen clearly in the reduced scatter in each of the plots. In general, predictions during the morning and evening peaks showed greater improvement than other times of the day. The best and worst correlation coefficients using the historical hourly activity profile are 0.653 and 0.071, respectively.

This sensitivity test demonstrates that improving the activity level characterization can lead to significant improvement in model comparison with observations. It is anticipated that additional improvement would be seen using day- and hour-specific vehicle traffic volumes for both light-duty and heavy-duty vehicles.

5. Discussion and Recommendations

The dispersion of pollutants from emission sources and resulting ambient concentrations of those pollutants depend on several factors—most importantly, atmospheric mixing and transport and emission strength. Air quality models predict ambient concentrations by parameterizing important atmospheric processes, using input data on emissions and meteorology. Therefore, the discrepancies between model-predicted and monitored concentrations are often attributed to deficiencies in a model's capability to characterize atmospheric processes or uncertainties in meteorological or emission inputs.

AERMOD, the model used in this analysis, is the current regulatory general-purpose air quality dispersion model. However, concerns have been raised by Caltrans and others about the appropriateness of using the AERMOD dispersion model for air quality modeling in the near-roadway environment. While the U.S. Environmental Protection Agency (EPA) considers the AERMOD dispersion model as its recommended near-field air quality dispersion model, the model has undergone only limited near-field (<100 m) model evaluation studies for near-ground level sources⁷ and its accuracy in predicting ambient concentrations needs further study to assure the community of its capabilities.

As presented in the previous section, significant discrepancies exist between model-predicted and monitored concentrations for locations in the vicinity of the I-710. Earlier studies have produced similar results. For example, in a study sponsored by National Academy of Sciences National Cooperative Highway Research Program (NCHRP 25-6), poor correlation was found between modeled predictions and near-roadway ambient CO measurements (see Figure 12). In another important study, the Route 9a study,⁸ comparisons between modeled and monitored data from that study were used by EPA as the basis for selecting the near roadway air dispersion model, CAL3QHC, as the guideline model for CO hotspot assessments. In the Route 9a study, the CAL3QHC model had a Pearson Correlation Coefficient of only 0.232 for data paired in location and time, even with information on hourly specific traffic volume, fleet mix, and speeds. Note, however, that substantial improvements have been made to emission factors models since these studies, and significantly higher correlations might be expected if these same studies were done today.

Despite the above findings, it is likely that a better correlation between modeled and monitored data can be significantly improved in future efforts if the following information is incorporated into the study:

Emissions Data: As discussed in the previous section, model-predicted concentrations lack the temporal variation that is present in monitored data. The lack of hourly temporal resolution detail in the input data to the model along with uncertainty in actual hour-to-hour truck and car volumes in the input data plays an important role in the actual emission source strength. Therefore, at a minimum the temporal variation of emissions needs to be better characterized for input to the model, to more credibly assess model performance. It is likely that the largest source of uncertainty

⁷ Of the more than dozen model evaluation databases used in AERMOD performance evaluation only the Prairie Grass study looked at near-surface, non-buoyant tracer releases in a flat area and none in an urban environment.

⁸ Evaluation of CO Intersection Modeling Techniques Using a New York City Database, Sigma Research Corporation prepared under contract to USEP/OAQPS, Contract No. 68D90067, WA 3-2, January, 1992.

is the emission source strength. Sensitivity testing using the Caltrans weigh-in-motion data suggested significant improvement in the model-to-monitor comparison using hour-by-hour traffic volumes. Future evaluations of model-to-monitor performance should include detailed information on traffic volumes for both light-duty vehicles and heavy-duty trucks along with speed profile information, because speeds and variations in speed also play an important role in motor vehicle emission rates.

Source Characterization: Roadway sources are currently characterized using the volume source model within AERMOD. However, for near-field assessment, impacts may be aliased if volume sources are too widely separated. It is recommended for very near-source impact assessment (< 100 m) that emissions sources be modeled as area sources.

On-site monitoring data: Collection of QA/QC meteorological data at both the background and downwind receptor location would reduce the uncertainty associated with the meteorological inputs to the model.

Background concentrations: In this analysis, monitored concentrations are adjusted for the background concentration in order to estimate the contribution from roadway sources only. This adjustment was done by subtracting the measured concentration at Del Amo site, which is assumed to be representative of the regional background concentrations. The assumption that this site is representative of the background concentration may also contribute to some of the differences between model-predicted and monitored concentrations, but is likely small relative to the other improvements discussed.

Until the inputs to the AERMOD model can be well characterized with reasonably small uncertainty, questions on the model's capability to clearly simulate near-roadway concentrations will remain unclear and results from the near-roadway air quality modeling are probably best used to provide information on an estimated change in concentration rather than absolute concentration under a proposed action.

EPA recognizes a number of these uncertainties in near roadway modeling and has begun efforts through its Office of Research and Development under the Clear Air Research multiyear plan to emphasize air research to better understand the linkages between traffic pollutant sources, atmospheric transport, and dispersion of emissions within the first few hundred meters of the roadway. A major data collection study on the near roadway exposure and effects from urban pollutants study was completed earlier this year in Detroit, Michigan⁹. The study includes wind tunnel simulations of flow and dispersion near roadway configurations to support the development and evaluation of a near roadway version of the AERMOD model, AERLINE, for application in urban, near-road studies and assist in the interpretation of site-specific monitoring. Findings and results from this study should become available over the next several years.

Pending results from this and other near-roadway studies, it is recommended that—in order to improve confidence in the application of the AERMOD model in the near-roadway environment—a permanent near-roadway air quality monitoring station be installed and maintained along the I-710 (perhaps near

⁹ <http://www.epa.gov/midwestcleandiesel/publications/webinars.html>

the weigh-in-motion station). The monitoring station would not only collect air quality data (both upwind and downwind) but at least hourly resolution traffic data (volumes by vehicle type, speeds, and speed profiles) and meteorological data (wind speed, direction, solar radiation, temperature, and humidity). This would aid not only in improving air quality modeling but also would provide a way to potentially measure the effects of proposed Early Action measures and future air quality action improvements directed at traffic along the I-710.

Figure 1. Locations of the Air Quality (East, West, and Del Amo) and Meteorological Monitoring Station (Long Beach) from the SCAQMD Dataset



Figure 2. Two Locations of the Air Quality (Monitor 1 and 2) and SCAQMD Meteorological Monitoring Station (Compton) from the Ning et al. (2010)



Figure 3. Scatter Plot of Model-Predicted and Monitored CO Concentrations

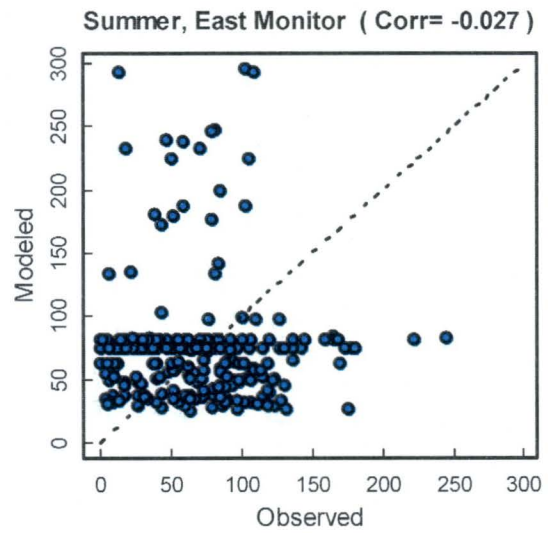
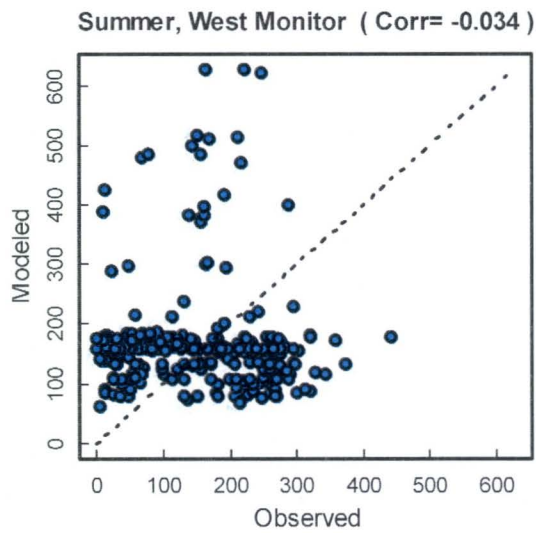
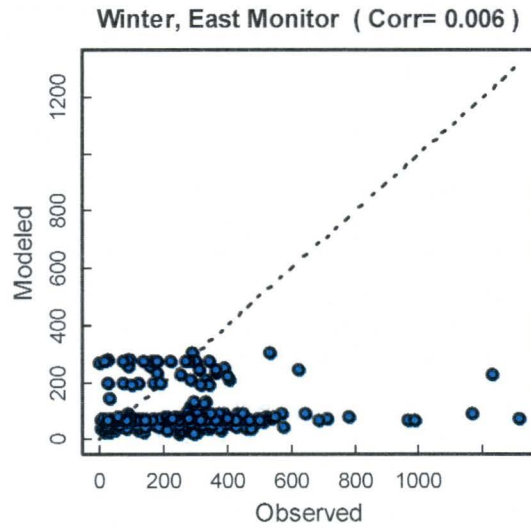
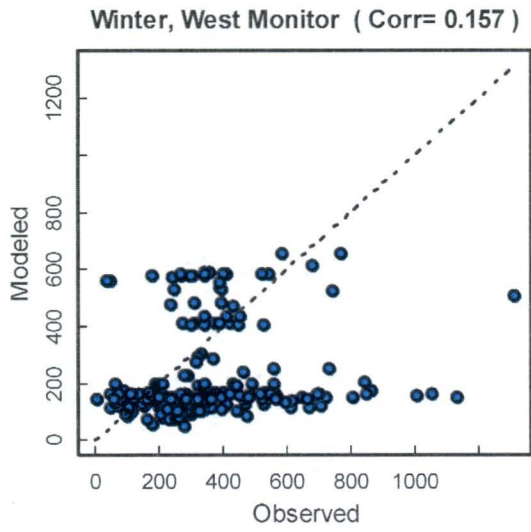


Figure 4. Scatter Plot of Model-Predicted and Monitored NO_x Concentrations

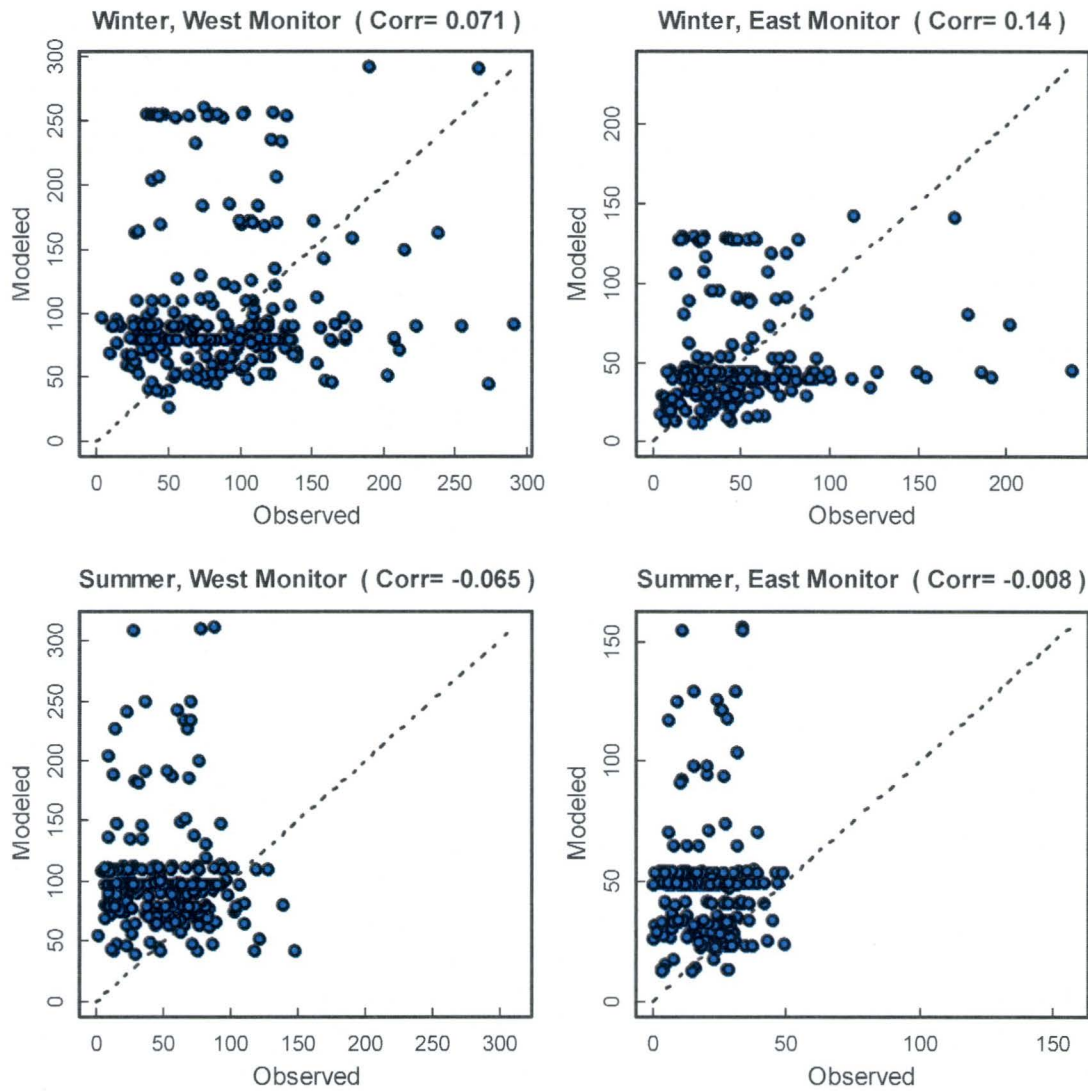


Figure 5. Scatter Plot of Model-Predicted and Monitored CO Concentration for Intra-Day Periods during Summer

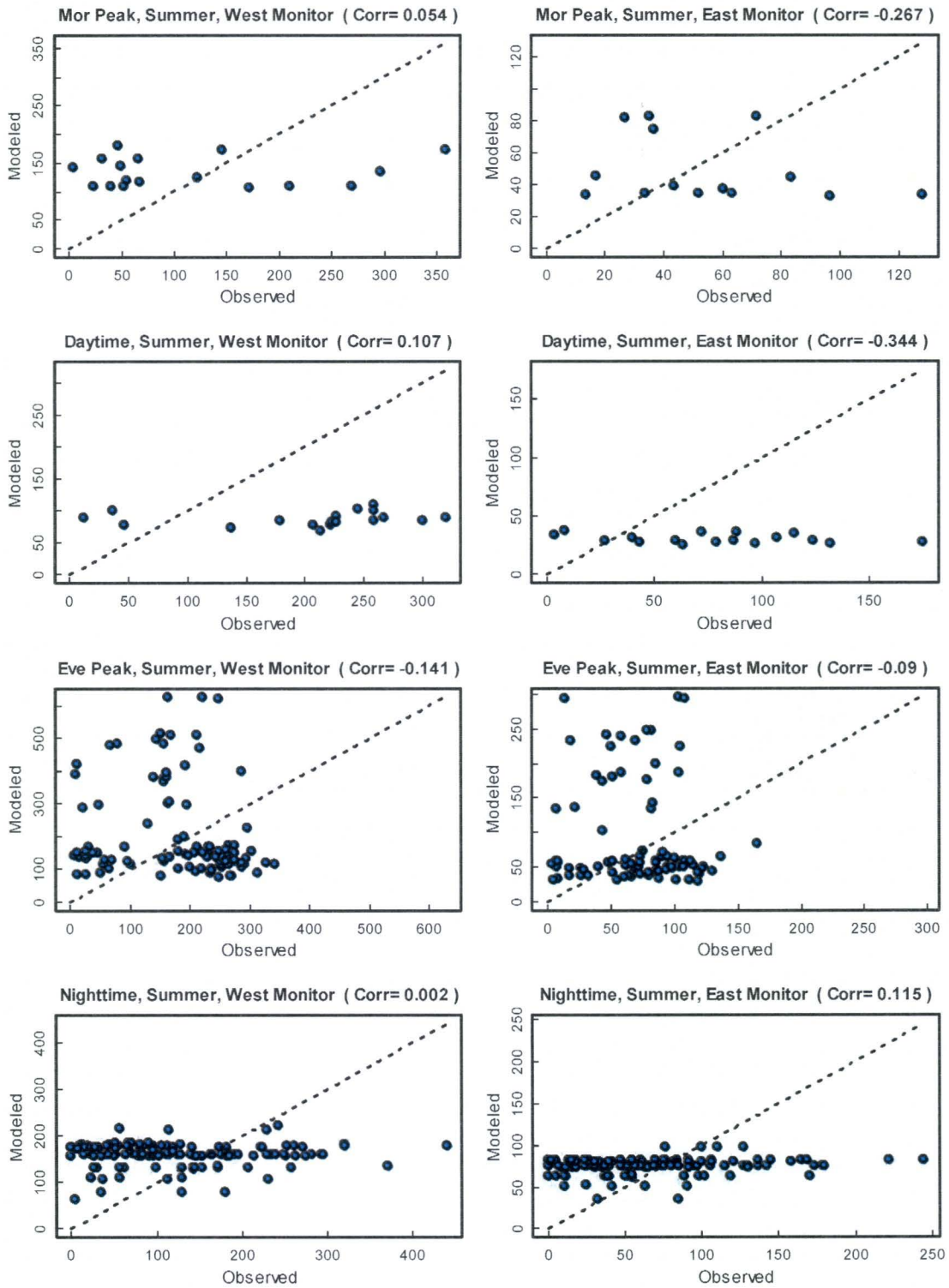


Figure 6. Scatter Plot of Model-Predicted and Monitored CO Concentrations for Intra-Day Periods during Winter

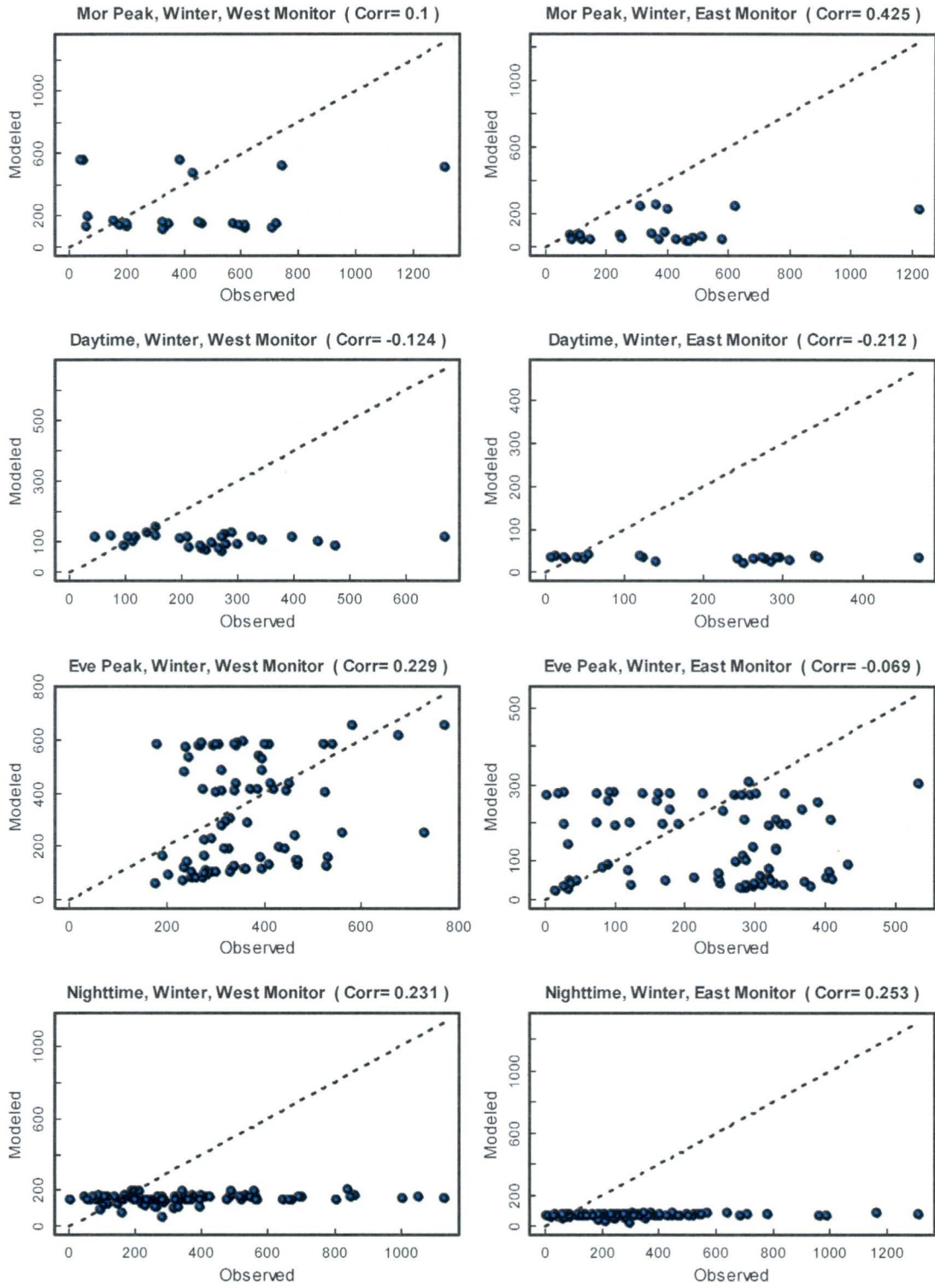


Figure 7. Scatter Plot of Model-Predicted and Monitored NO_x Concentrations for Intra-Day Periods during Summer

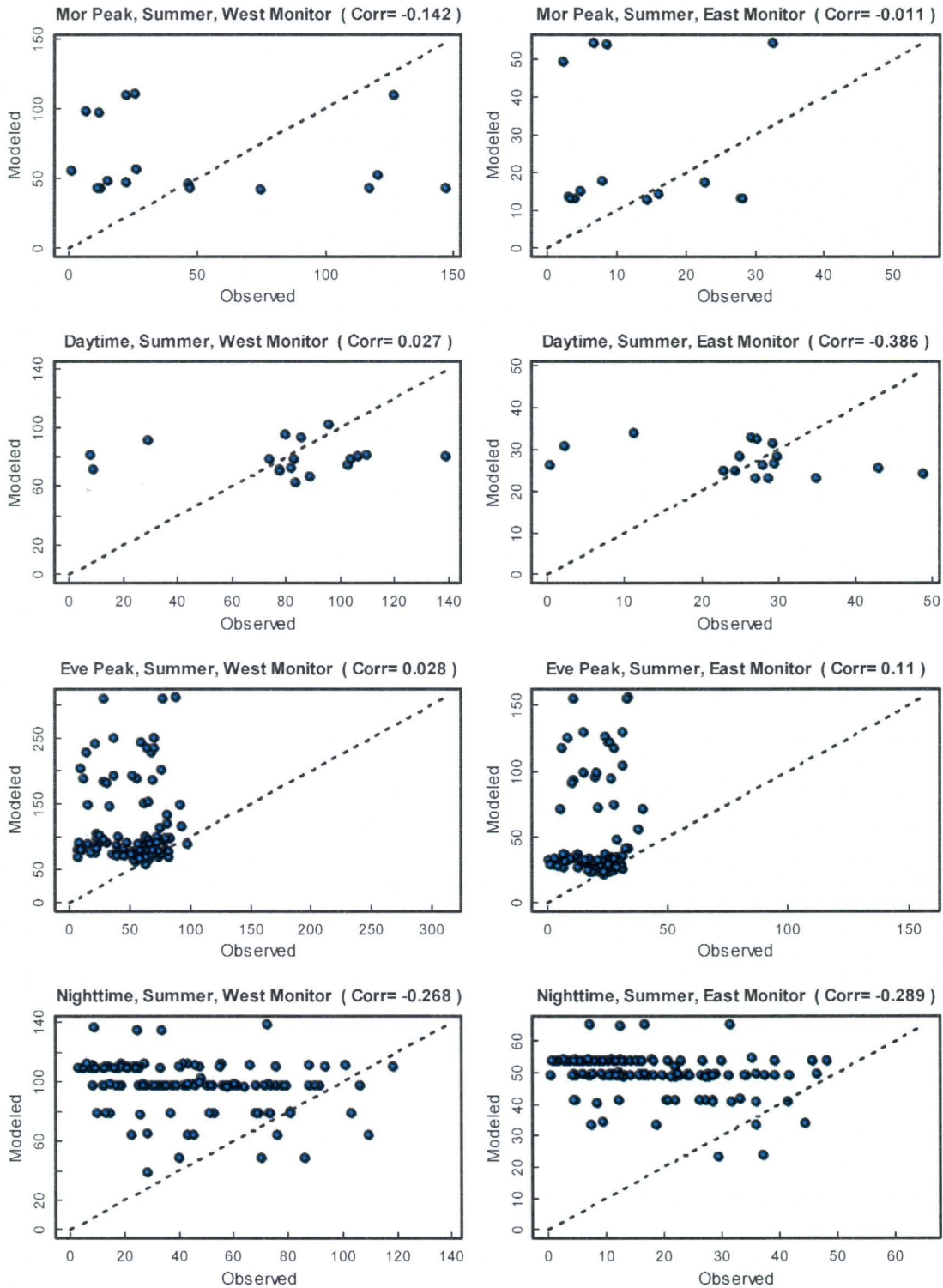


Figure 8. Scatter Plots of Model-Predicted and Monitored NO_x Concentrations for Intra-Day Periods during Winter

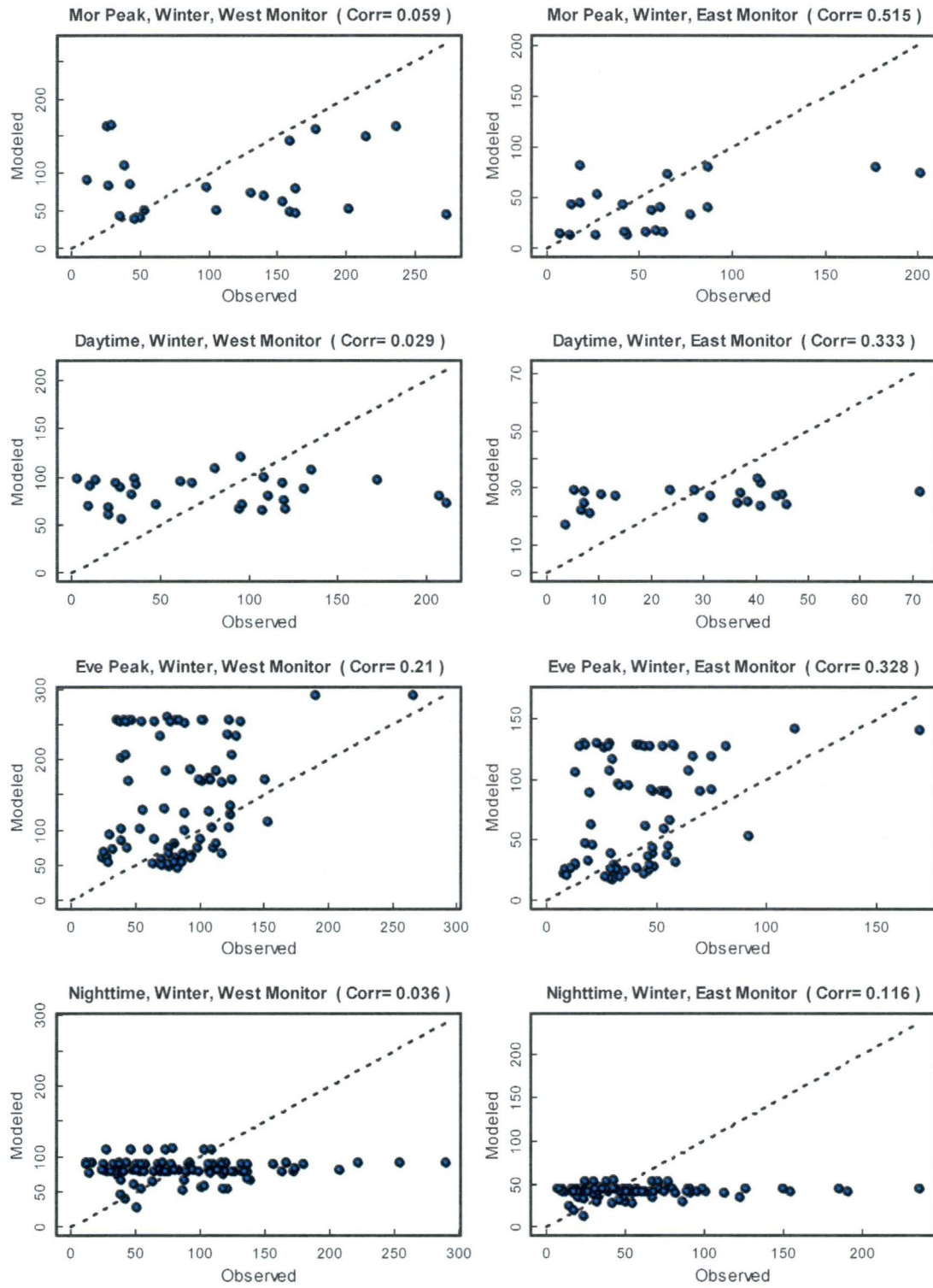


Table 1. Pearson Correlation Coefficients between Model-Predicted and Monitored Concentrations Hourly Concentrations

| | CO | | | | NO _x | | | |
|-----------------|--------|--------|--------|--------|-----------------|--------|--------|-------|
| | Summer | | Winter | | Summer | | Winter | |
| | West | East | West | East | West | East | West | East |
| Morning Peak | 0.054 | -0.267 | 0.100 | 0.425 | -0.142 | -0.011 | 0.059 | 0.515 |
| Daytime Hours | 0.107 | -0.344 | -0.124 | -0.212 | 0.027 | -0.386 | 0.029 | 0.333 |
| Evening Peak | -0.141 | -0.090 | 0.229 | -0.069 | 0.028 | 0.110 | 0.210 | 0.328 |
| Nighttime Hours | 0.002 | 0.115 | 0.231 | 0.253 | -0.268 | -0.289 | 0.036 | 0.116 |
| All | -0.034 | -0.027 | 0.157 | 0.006 | -0.065 | -0.008 | 0.071 | 0.140 |

Table 2. Pearson Correlation Coefficients between Model-Predicted and Monitored Hourly Concentrations Using the "Best Receptor" Parallel to the Roadway

| | CO | | | | NO _x | | | |
|-----------------|--------|--------|--------|--------|-----------------|--------|--------|-------|
| | Summer | | Winter | | Summer | | Winter | |
| | West | East | West | East | West | East | West | East |
| Morning Peak | 0.187 | -0.260 | 0.167 | 0.425 | -0.105 | -0.009 | 0.097 | 0.521 |
| Daytime Hours | 0.262 | -0.321 | -0.075 | -0.186 | 0.188 | -0.379 | 0.154 | 0.349 |
| Evening Peak | -0.115 | -0.082 | 0.245 | -0.052 | 0.036 | 0.110 | 0.219 | 0.332 |
| Nighttime Hours | 0.208 | 0.158 | 0.297 | 0.260 | -0.254 | -0.286 | 0.126 | 0.143 |
| All | 0.011 | -0.018 | 0.179 | 0.013 | -0.054 | -0.007 | 0.093 | 0.146 |

Figure 9. Q-Q Plot between Model-Predicted and Monitored Concentrations (PPB) during Summer

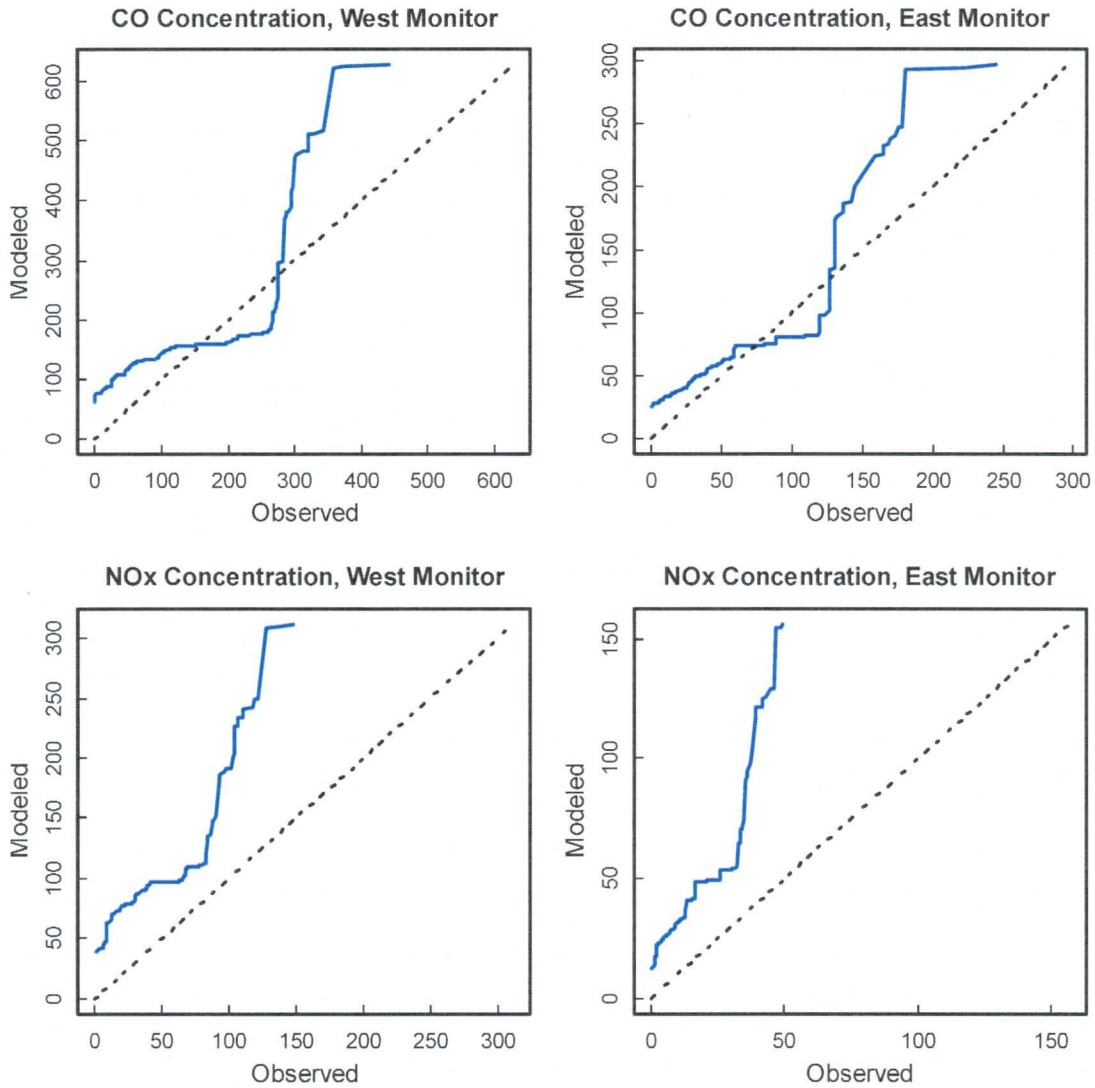


Figure 10. Q-Q Plot between Model-Predicted and Monitored Hourly Concentrations (PPB) during Winter

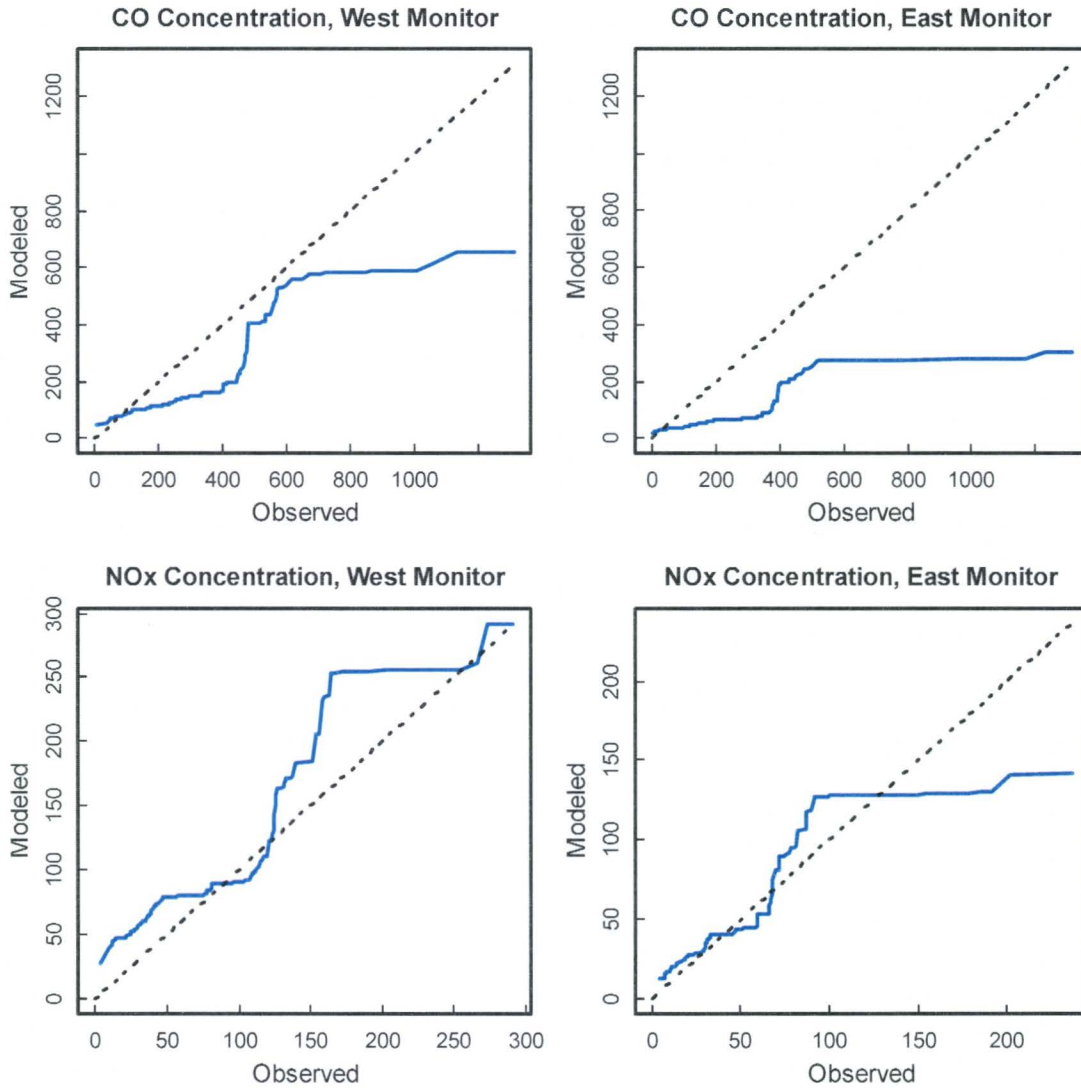


Figure 11. Comparison of Model-Predicted and Monitored Concentration Distributions (PPB) for Model Predictions, Based on 75 Receptors in the Vicinity of Monitoring Location

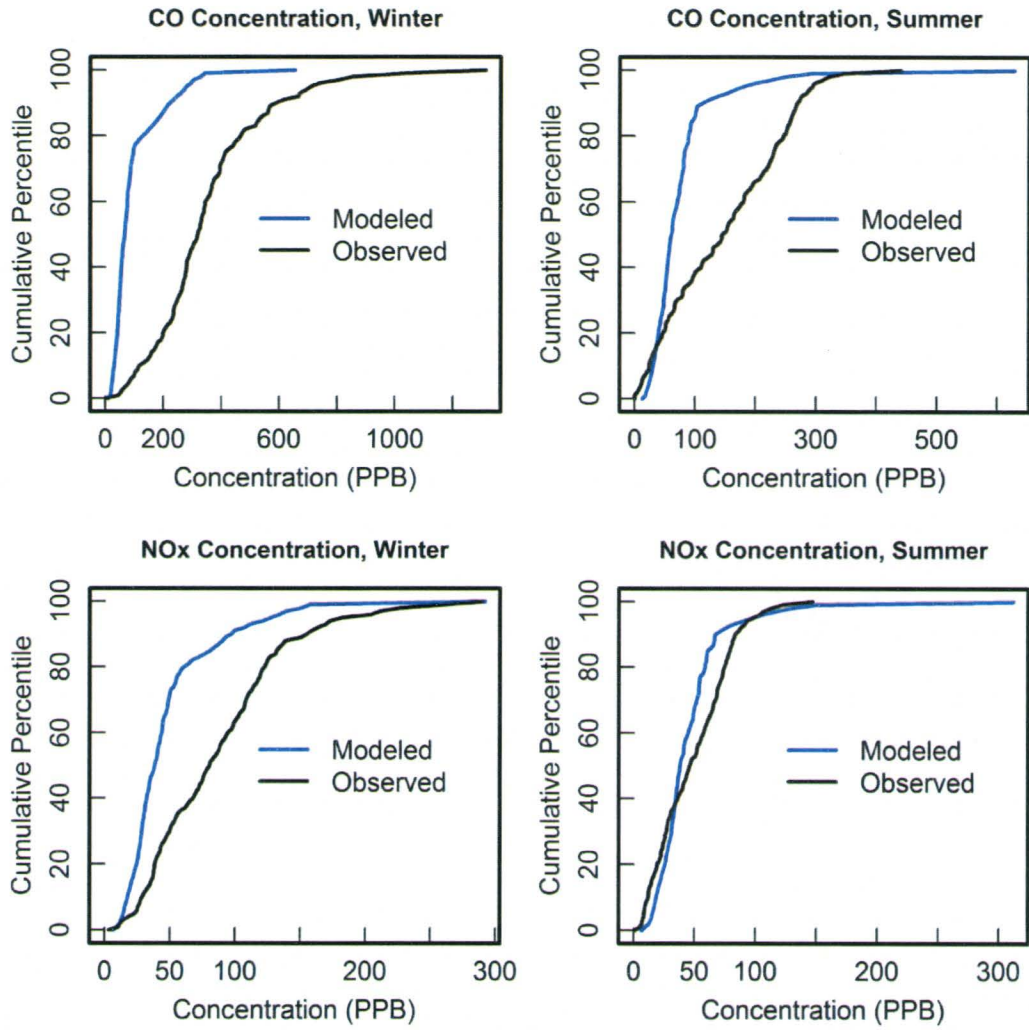


Figure 12. Comparison of Predicted Concentrations by CAL3QHC and Monitored CO Concentrations at Three at Elizabeth, NJ, and St. Paul MN, in a NCHRP Study

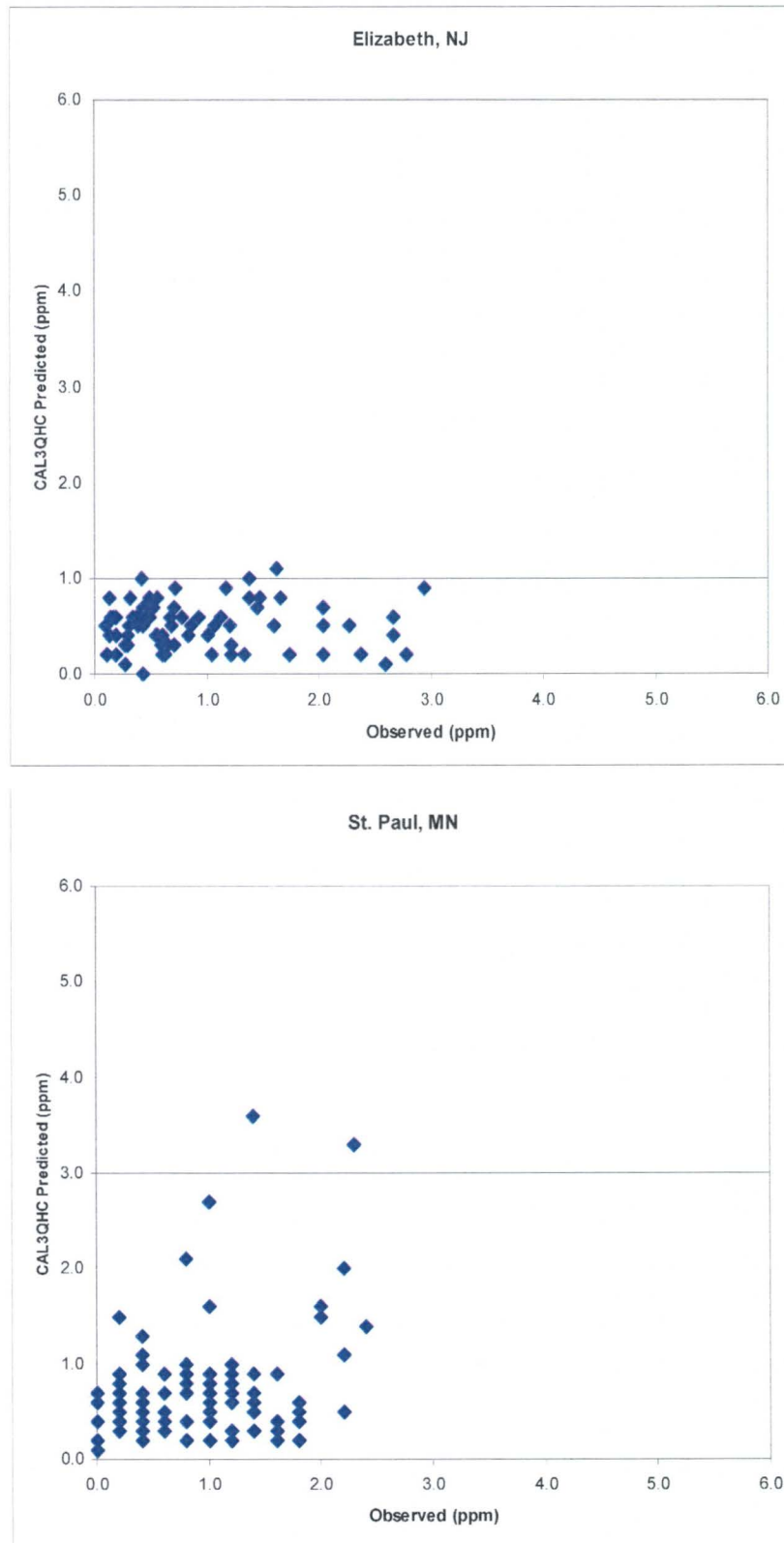


Table 3. Comparison of Average, Median, 10th Percentile, and 90th Percentile of Model-Predicted and Monitored CO Concentrations (PPB)

| Period | Season | Site | Sample Size | 10th Percentile (Monitored) | 10th Percentile (Modeled) | Average (Monitored) | Average (Modeled) | Median (Monitored) | Median (Modeled) | 90th Percentile (Monitored) | 90th Percentile (Modeled) |
|------------------|---------------|-------------|-------------|-----------------------------|---------------------------|---------------------|-------------------|--------------------|------------------|-----------------------------|---------------------------|
| Daytime Hours | Winter | East | 22 | 23.00 | 26.27 | 192.59 | 33.22 | 246.50 | 34.07 | 340.00 | 37.63 |
| Evening Peak | Winter | East | 78 | 34.00 | 34.87 | 229.51 | 147.06 | 275.50 | 129.93 | 379.00 | 275.67 |
| Morning Peak | Winter | East | 22 | 103.00 | 39.53 | 369.05 | 97.54 | 369.00 | 66.47 | 578.00 | 246.17 |
| Nighttime Hours | Winter | East | 100 | 75.50 | 57.17 | 309.64 | 70.34 | 274.00 | 70.32 | 543.50 | 76.90 |
| All Hours | Winter | East | 222 | 54.00 | 35.12 | 275.77 | 96.31 | 274.00 | 69.96 | 475.00 | 246.72 |
| Daytime Hours | Winter | West | 30 | 100.00 | 79.67 | 246.93 | 103.92 | 239.00 | 109.63 | 420.00 | 126.78 |
| Evening Peak | Winter | West | 80 | 239.50 | 99.40 | 361.71 | 328.88 | 340.00 | 289.14 | 526.50 | 583.07 |
| Morning Peak | Winter | West | 24 | 60.00 | 118.81 | 411.46 | 239.33 | 367.00 | 150.91 | 722.00 | 553.22 |
| Nighttime Hours | Winter | West | 102 | 102.00 | 122.79 | 350.01 | 150.83 | 317.00 | 149.32 | 670.00 | 170.98 |
| All Hours | Winter | West | 236 | 117.00 | 100.49 | 347.12 | 214.22 | 318.50 | 149.77 | 594.00 | 537.86 |
| Daytime Hours | Summer | East | 17 | 8.33 | 26.15 | 77.55 | 30.67 | 78.33 | 29.26 | 131.67 | 36.64 |
| Evening Peak | Summer | East | 89 | 13.33 | 35.13 | 72.46 | 89.42 | 78.33 | 55.71 | 118.33 | 232.69 |
| Morning Peak | Summer | East | 14 | 16.67 | 33.36 | 54.29 | 49.25 | 47.50 | 37.94 | 96.67 | 82.18 |
| Nighttime Hours | Summer | East | 137 | 11.67 | 62.96 | 65.61 | 75.05 | 56.67 | 75.01 | 130.00 | 81.63 |
| All Hours | Summer | East | 257 | 13.33 | 34.56 | 68.15 | 75.69 | 65.00 | 74.49 | 121.67 | 97.99 |
| Daytime Hours | Summer | West | 18 | 36.67 | 73.41 | 201.94 | 87.14 | 225.00 | 85.28 | 300.00 | 102.43 |
| Evening Peak | Summer | West | 103 | 26.67 | 97.59 | 179.83 | 206.61 | 198.33 | 147.06 | 281.67 | 472.29 |
| Morning Peak | Summer | West | 17 | 23.33 | 107.95 | 117.84 | 133.60 | 65.00 | 124.70 | 296.67 | 173.30 |
| Nighttime Hours | Summer | West | 141 | 20.00 | 132.18 | 120.38 | 159.75 | 103.33 | 160.06 | 250.00 | 179.55 |
| All Hours | Summer | West | 279 | 23.33 | 93.93 | 147.43 | 170.77 | 145.00 | 157.91 | 271.67 | 222.38 |

Table 4. Comparison of Average, Median, 10th Percentile and 90th Percentile of Model-Predicted and Monitored NO_x Concentrations (PPB)

| Period | Season | Site | Sample Size | 10th Percentile (Monitored) | 10th Percentile (Modeled) | Average (Monitored) | Average (Modeled) | Median (Monitored) | Median (Modeled) | 90th Percentile (Monitored) | 90th Percentile (Modeled) |
|------------------|---------------|-------------|-------------|-----------------------------|---------------------------|---------------------|-------------------|--------------------|------------------|-----------------------------|---------------------------|
| Daytime Hours | Winter | East | 22 | 6.50 | 20.76 | 28.00 | 26.15 | 30.67 | 27.16 | 45.20 | 29.27 |
| Evening Peak | Winter | East | 78 | 13.33 | 20.13 | 41.02 | 69.71 | 36.49 | 60.02 | 66.60 | 128.22 |
| Morning Peak | Winter | East | 22 | 13.26 | 13.35 | 58.23 | 38.76 | 48.64 | 38.57 | 87.00 | 80.53 |
| Nighttime Hours | Winter | East | 100 | 17.42 | 32.89 | 55.40 | 40.89 | 49.40 | 40.79 | 96.74 | 44.82 |
| All Hours | Winter | East | 222 | 13.25 | 21.34 | 47.91 | 49.34 | 42.26 | 40.45 | 86.65 | 106.88 |
| Daytime Hours | Winter | West | 30 | 11.99 | 65.37 | 78.35 | 84.53 | 74.28 | 88.41 | 153.41 | 102.50 |
| Evening Peak | Winter | West | 80 | 38.10 | 55.68 | 84.57 | 149.29 | 82.01 | 128.86 | 124.43 | 255.67 |
| Morning Peak | Winter | West | 24 | 26.89 | 41.63 | 114.00 | 86.95 | 118.42 | 76.09 | 214.24 | 162.98 |
| Nighttime Hours | Winter | West | 102 | 31.92 | 64.69 | 84.62 | 81.83 | 73.91 | 80.17 | 138.89 | 91.56 |
| All Hours | Winter | West | 236 | 28.04 | 53.80 | 86.80 | 105.56 | 80.45 | 86.32 | 156.13 | 206.11 |
| Daytime Hours | Summer | East | 17 | 0.00 | 22.93 | 25.82 | 27.23 | 27.21 | 26.26 | 42.97 | 32.51 |
| Evening Peak | Summer | East | 89 | 0.00 | 24.83 | 20.11 | 49.93 | 21.89 | 32.09 | 31.24 | 121.59 |
| Morning Peak | Summer | East | 14 | 2.33 | 12.91 | 13.05 | 25.34 | 8.28 | 14.73 | 28.13 | 54.29 |
| Nighttime Hours | Summer | East | 137 | 5.98 | 41.13 | 17.56 | 49.42 | 14.32 | 49.37 | 35.22 | 53.92 |
| All Hours | Summer | East | 257 | 3.12 | 24.79 | 18.74 | 46.82 | 18.51 | 48.95 | 32.69 | 65.03 |
| Daytime Hours | Summer | West | 18 | 9.07 | 66.67 | 79.80 | 79.19 | 83.38 | 78.11 | 109.60 | 94.68 |
| Evening Peak | Summer | West | 103 | 11.91 | 69.64 | 50.43 | 114.02 | 55.46 | 87.52 | 80.12 | 226.12 |
| Morning Peak | Summer | West | 17 | 6.29 | 42.29 | 49.09 | 63.57 | 25.76 | 47.55 | 126.90 | 109.34 |
| Nighttime Hours | Summer | West | 141 | 12.27 | 78.79 | 43.03 | 97.83 | 40.25 | 97.44 | 78.84 | 110.61 |
| All Hours | Summer | West | 279 | 11.87 | 65.69 | 48.51 | 100.52 | 45.92 | 97.08 | 83.56 | 134.90 |

Table 5. Statistical Comparison of Model-Predicted and Monitored Hourly CO Concentrations (PPB)

| Period | Season | Site | Sample Size | Average Bias | Average Absolute Bias | Std Deviation of Bias | Fractional Bias |
|------------------|---------------|-------------|-------------|----------------|-----------------------|-----------------------|-----------------|
| Daytime Hours - | Winter | East | 22 | -159.38 | 166.05 | 137.24 | -1.41 |
| Evening Peak | Winter | East | 78 | -82.45 | 152.51 | 166.23 | -0.44 |
| Morning Peak | Winter | East | 22 | -271.50 | 271.50 | 231.28 | -1.16 |
| Nighttime Hours | Winter | East | 100 | -239.30 | 244.62 | 230.34 | -1.26 |
| All Hours | Winter | East | 222 | -179.46 | 207.13 | 214.69 | -0.96 |
| Daytime Hours | Winter | West | 30 | -143.02 | 151.61 | 135.07 | -0.82 |
| Evening Peak | Winter | West | 80 | -32.83 | 178.89 | 206.95 | -0.10 |
| Morning Peak | Winter | West | 24 | -172.13 | 293.37 | 326.73 | -0.53 |
| Nighttime Hours | Winter | West | 102 | -199.18 | 219.26 | 225.09 | -0.80 |
| All Hours | Winter | West | 236 | -132.90 | 204.51 | 233.15 | -0.47 |
| Daytime Hours | Summer | East | 17 | -46.88 | 54.23 | 47.17 | -0.87 |
| Evening Peak | Summer | East | 89 | 16.96 | 66.38 | 85.84 | 0.21 |
| Morning Peak | Summer | East | 14 | -5.04 | 33.69 | 42.85 | -0.10 |
| Nighttime Hours | Summer | East | 137 | 9.44 | 39.21 | 48.13 | 0.13 |
| All Hours | Summer | East | 257 | 7.53 | 49.31 | 65.07 | 0.10 |
| Daytime Hours (| Summer | West | 18 | -114.80 | 134.16 | 88.22 | -0.79 |
| Evening Peak | Summer | West | 103 | 26.78 | 148.98 | 179.76 | 0.14 |
| Morning Peak | Summer | West | 17 | 15.76 | 95.07 | 108.98 | 0.13 |
| Nighttime Hours | Summer | West | 141 | 39.37 | 84.54 | 91.92 | 0.28 |
| All Hours | Summer | West | 279 | 23.34 | 112.17 | 136.55 | 0.15 |

Table 6. Statistical Comparison of Model-Predicted and Monitored Hourly NO_x Concentrations (PPB)

| Period | Season | Site | Sample Size | Average Bias | Average Absolute Bias | Std Deviation of Bias | Fractional Bias |
|------------------|---------------|-------------|-------------|--------------|-----------------------|-----------------------|-----------------|
| Daytime Hours - | Winter | East | 22 | -1.85 | 14.75 | 17.25 | -0.07 |
| Evening Peak | Winter | East | 78 | 28.68 | 39.16 | 42.90 | 0.52 |
| Morning Peak | Winter | East | 22 | -19.46 | 33.96 | 41.82 | -0.40 |
| Nighttime Hours | Winter | East | 100 | -14.51 | 28.66 | 40.00 | -0.30 |
| All Hours | Winter | East | 222 | 1.43 | 31.50 | 44.43 | 0.03 |
| Daytime Hours | Winter | West | 30 | 6.18 | 51.18 | 60.00 | 0.08 |
| Evening Peak | Winter | West | 80 | 64.71 | 78.73 | 81.86 | 0.55 |
| Morning Peak | Winter | West | 24 | -27.05 | 70.99 | 87.01 | -0.27 |
| Nighttime Hours | Winter | West | 102 | -2.78 | 42.39 | 54.09 | -0.03 |
| All Hours | Winter | West | 236 | 18.77 | 58.73 | 76.49 | 0.20 |
| Daytime Hours | Summer | East | 17 | 1.42 | 9.75 | 14.02 | 0.05 |
| Evening Peak | Summer | East | 89 | 29.82 | 30.34 | 37.35 | 0.85 |
| Morning Peak | Summer | East | 14 | 12.29 | 17.80 | 21.18 | 0.64 |
| Nighttime Hours | Summer | East | 137 | 31.86 | 32.35 | 14.85 | 0.95 |
| All Hours | Summer | East | 257 | 28.07 | 29.37 | 26.48 | 0.86 |
| Daytime Hours (| Summer | West | 18 | -0.61 | 26.09 | 35.03 | -0.01 |
| Evening Peak | Summer | West | 103 | 63.59 | 64.61 | 65.81 | 0.77 |
| Morning Peak | Summer | West | 17 | 14.48 | 50.25 | 59.52 | 0.26 |
| Nighttime Hours | Summer | West | 141 | 54.80 | 57.12 | 34.81 | 0.78 |
| All Hours | Summer | West | 279 | 52.01 | 57.47 | 52.89 | 0.70 |

Table 7. Distribution of the Ratio of Model-Predicted to Monitored CO Concentrations (PPB)

| Period | Season | Site | Sample Size | Mean Ratio | Median Ratio | 75th Percentile Ratio | 90th Percentile Ratio | 95th Percentile Ratio |
|------------------|---------------|-------------|-------------|-------------|--------------|-----------------------|-----------------------|-----------------------|
| Daytime Hours | Winter | East | 22 | 0.69 | 0.13 | 0.77 | 1.58 | 2.89 |
| Evening Peak | Winter | East | 78 | 2.41 | 0.64 | 1.29 | 2.84 | 7.30 |
| Morning Peak | Winter | East | 22 | 0.35 | 0.26 | 0.56 | 0.70 | 0.79 |
| Nighttime Hours | Winter | East | 100 | 0.62 | 0.26 | 0.46 | 0.88 | 1.73 |
| All Hours | Winter | East | 222 | 1.23 | 0.31 | 0.80 | 1.58 | 2.84 |
| Daytime Hours | Winter | West | 30 | 0.60 | 0.38 | 0.88 | 1.06 | 1.60 |
| Evening Peak | Winter | West | 80 | 0.96 | 0.85 | 1.36 | 1.95 | 2.17 |
| Morning Peak | Winter | West | 24 | 1.77 | 0.46 | 1.08 | 3.20 | 11.65 |
| Nighttime Hours | Winter | West | 102 | 1.38 | 0.46 | 0.86 | 1.45 | 1.94 |
| All Hours | Winter | West | 236 | 1.18 | 0.50 | 1.02 | 1.72 | 2.19 |
| Daytime Hours | Summer | East | 17 | 1.25 | 0.40 | 0.65 | 4.50 | 10.21 |
| Evening Peak | Summer | East | 89 | 2.46 | 0.81 | 2.86 | 6.25 | 8.70 |
| Morning Peak | Summer | East | 14 | 1.34 | 0.97 | 2.35 | 2.72 | 3.06 |
| Nighttime Hours | Summer | East | 137 | 3.21 | 1.25 | 2.48 | 5.43 | 11.22 |
| All Hours | Summer | East | 257 | 2.71 | 1.09 | 2.44 | 5.41 | 8.93 |
| Daytime Hours | Summer | West | 18 | 0.99 | 0.38 | 0.47 | 2.73 | 7.72 |
| Evening Peak | Summer | West | 103 | 2.95 | 0.79 | 2.52 | 5.85 | 10.37 |
| Morning Peak | Summer | West | 17 | 4.41 | 2.09 | 3.01 | 4.97 | 42.67 |
| Nighttime Hours | Summer | West | 141 | 3.65 | 1.54 | 2.95 | 6.42 | 12.43 |
| All Hours | Summer | West | 279 | 3.26 | 1.25 | 2.73 | 5.95 | 10.74 |

Table 8. Distribution of the Ratio of Model-Predicted to Monitored NO_x Concentrations (PPB)

| Period | Season | Site | Sample Size | Mean Ratio | Median Ratio | 75th Percentile Ratio | 90th Percentile Ratio | 95th Percentile Ratio |
|------------------|---------------|-------------|-------------|-------------|--------------|-----------------------|-----------------------|-----------------------|
| Daytime Hours | Winter | East | 22 | 1.74 | 0.84 | 2.68 | 4.04 | 4.58 |
| Evening Peak | Winter | East | 78 | 2.18 | 1.64 | 2.70 | 4.55 | 7.77 |
| Morning Peak | Winter | East | 22 | 1.07 | 0.56 | 1.11 | 2.48 | 3.18 |
| Nighttime Hours | Winter | East | 100 | 1.21 | 0.79 | 1.46 | 2.27 | 3.59 |
| All Hours | Winter | East | 222 | 1.59 | 0.93 | 2.08 | 3.39 | 4.60 |
| Daytime Hours | Winter | West | 30 | 3.05 | 1.36 | 2.90 | 7.16 | 8.54 |
| Evening Peak | Winter | West | 80 | 2.15 | 1.67 | 2.66 | 5.07 | 5.89 |
| Morning Peak | Winter | West | 24 | 1.64 | 0.82 | 1.56 | 5.58 | 6.25 |
| Nighttime Hours | Winter | West | 102 | 1.52 | 1.07 | 1.86 | 2.59 | 3.97 |
| All Hours | Winter | West | 236 | 1.94 | 1.17 | 2.36 | 3.93 | 6.16 |
| Daytime Hours | Summer | East | 17 | 6.60 | 1.01 | 1.19 | 13.04 | 83.36 |
| Evening Peak | Summer | East | 89 | 4.15 | 1.57 | 4.70 | 10.19 | 15.71 |
| Morning Peak | Summer | East | 14 | 4.17 | 2.69 | 4.30 | 8.20 | 22.11 |
| Nighttime Hours | Summer | East | 137 | 7.13 | 3.45 | 6.16 | 11.29 | 29.28 |
| All Hours | Summer | East | 257 | 5.90 | 2.68 | 4.92 | 11.03 | 19.24 |
| Daytime Hours | Summer | West | 18 | 1.89 | 0.91 | 1.09 | 7.89 | 10.03 |
| Evening Peak | Summer | West | 103 | 3.67 | 1.76 | 4.05 | 10.54 | 11.15 |
| Morning Peak | Summer | West | 17 | 6.72 | 2.13 | 4.29 | 15.49 | 62.25 |
| Nighttime Hours | Summer | West | 141 | 4.21 | 2.60 | 5.26 | 8.51 | 13.07 |
| All Hours | Summer | West | 279 | 4.01 | 2.14 | 4.44 | 9.06 | 12.84 |

Table 9. Comparison of Average, Median, 10th Percentile, and 90th Percentile of Best Model-Predicted CO Concentrations at Receptors Parallel to the Roadway and Monitored CO Concentrations (PPB)

| Period | Season | Site | Sample Size | 10th Percentile (Monitored) | 10th Percentile (Modeled) | Average (Monitored) | Average (Modeled) | Median (Monitored) | Median (Modeled) | 90th Percentile (Monitored) | 90th Percentile (Modeled) |
|------------------|---------------|-------------|-------------|-----------------------------|---------------------------|---------------------|-------------------|--------------------|------------------|-----------------------------|---------------------------|
| Daytime Hours | Winter | East | 22 | 23.00 | 26.51 | 192.59 | 33.28 | 246.50 | 34.21 | 340.00 | 37.75 |
| Evening Peak | Winter | East | 78 | 34.00 | 34.36 | 229.51 | 147.22 | 275.50 | 132.52 | 379.00 | 275.71 |
| Morning Peak | Winter | East | 22 | 103.00 | 40.20 | 369.05 | 98.41 | 369.00 | 67.04 | 578.00 | 247.16 |
| Nighttime Hours | Winter | East | 100 | 75.50 | 57.19 | 309.64 | 70.79 | 274.00 | 70.91 | 543.50 | 77.61 |
| All Hours | Winter | East | 222 | 54.00 | 35.25 | 275.77 | 96.66 | 274.00 | 70.55 | 475.00 | 248.31 |
| Daytime Hours | Winter | West | 30 | 100.00 | 82.00 | 246.93 | 104.34 | 239.00 | 108.51 | 420.00 | 127.19 |
| Evening Peak | Winter | West | 80 | 239.50 | 103.11 | 361.71 | 326.70 | 340.00 | 299.68 | 526.50 | 569.00 |
| Morning Peak | Winter | West | 24 | 60.00 | 121.68 | 411.46 | 233.63 | 367.00 | 154.92 | 722.00 | 495.44 |
| Nighttime Hours | Winter | West | 102 | 102.00 | 120.38 | 350.01 | 155.04 | 317.00 | 156.29 | 670.00 | 171.67 |
| All Hours | Winter | West | 236 | 117.00 | 100.68 | 347.12 | 214.78 | 318.50 | 156.27 | 594.00 | 518.32 |
| Daytime Hours | Summer | East | 17 | 8.33 | 26.20 | 77.55 | 30.73 | 78.33 | 29.21 | 131.67 | 36.84 |
| Evening Peak | Summer | East | 89 | 13.33 | 35.17 | 72.46 | 89.19 | 78.33 | 56.00 | 118.33 | 229.72 |
| Morning Peak | Summer | East | 14 | 16.67 | 33.08 | 54.29 | 49.10 | 47.50 | 38.30 | 96.67 | 81.41 |
| Nighttime Hours | Summer | East | 137 | 11.67 | 62.69 | 65.61 | 74.80 | 56.67 | 75.07 | 130.00 | 81.66 |
| All Hours | Summer | East | 257 | 13.33 | 34.24 | 68.15 | 75.47 | 65.00 | 73.90 | 121.67 | 98.44 |
| Daytime Hours | Summer | West | 18 | 36.67 | 74.36 | 201.94 | 87.02 | 225.00 | 86.04 | 300.00 | 103.70 |

| Period | Season | Site | Sample Size | 10th Percentile (Monitored) | 10th Percentile (Modeled) | Average (Monitored) | Average (Modeled) | Median (Monitored) | Median (Modeled) | 90th Percentile (Monitored) | 90th Percentile (Modeled) |
|------------------|---------------|-------------|-------------|-----------------------------|---------------------------|---------------------|-------------------|--------------------|------------------|-----------------------------|---------------------------|
| Evening Peak | Summer | West | 103 | 26.67 | 95.99 | 179.83 | 203.23 | 198.33 | 144.14 | 281.67 | 455.68 |
| Morning Peak | Summer | West | 17 | 23.33 | 105.34 | 117.84 | 131.31 | 65.00 | 121.94 | 296.67 | 171.90 |
| Nighttime Hours | Summer | West | 141 | 20.00 | 128.51 | 120.38 | 156.94 | 103.33 | 165.28 | 250.00 | 171.90 |
| All Hours | Summer | West | 279 | 23.33 | 94.03 | 147.43 | 167.96 | 145.00 | 153.19 | 271.67 | 223.35 |

Table 10. Comparison of Average, Median, 10th Percentile and 90th Percentile of Best Model-Predicted NO_x Concentration at Receptors Parallel to the Roadway and Monitored NO_x Concentrations (PPB)

| Period | Season | Site | Sample Size | 10th Percentile (Monitored) | 10th Percentile (Modeled) | Average (Monitored) | Average (Modeled) | Median (Monitored) | Median (Modeled) | 90th Percentile (Monitored) | 90th Percentile (Modeled) |
|------------------|---------------|-------------|-------------|-----------------------------|---------------------------|---------------------|-------------------|--------------------|------------------|-----------------------------|---------------------------|
| Daytime Hours | Winter | East | 22 | 6.50 | 20.65 | 28.00 | 26.09 | 30.67 | 27.08 | 45.20 | 29.07 |
| Evening Peak | Winter | East | 78 | 13.33 | 20.09 | 41.02 | 69.25 | 36.49 | 59.52 | 66.60 | 127.20 |
| Morning Peak | Winter | East | 22 | 13.26 | 13.38 | 58.23 | 38.73 | 48.64 | 38.78 | 87.00 | 80.30 |
| Nighttime Hours | Winter | East | 100 | 17.42 | 32.58 | 55.40 | 40.86 | 49.40 | 40.88 | 96.74 | 44.88 |
| All Hours | Winter | East | 222 | 13.25 | 21.44 | 47.91 | 49.16 | 42.26 | 40.61 | 86.65 | 105.89 |
| Daytime Hours | Winter | West | 30 | 11.99 | 64.08 | 78.35 | 82.52 | 74.28 | 86.17 | 153.41 | 101.23 |
| Evening Peak | Winter | West | 80 | 38.10 | 55.89 | 84.57 | 146.08 | 82.01 | 124.40 | 124.43 | 249.16 |
| Morning Peak | Winter | West | 24 | 26.89 | 41.19 | 114.00 | 86.66 | 118.42 | 78.09 | 214.24 | 155.56 |
| Nighttime Hours | Winter | West | 102 | 31.92 | 63.45 | 84.62 | 81.66 | 73.91 | 81.74 | 138.89 | 92.35 |
| All Hours | Winter | West | 236 | 28.04 | 55.14 | 86.80 | 104.11 | 80.45 | 84.34 | 156.13 | 202.48 |

Task 2b3: Data Analysis to Assess the Representativeness of Modeled Near-Roadway Concentrations–Final

| Period | Season | Site | Sample Size | 10th Percentile (Monitored) | 10th Percentile (Modeled) | Average (Monitored) | Average (Modeled) | Median (Monitored) | Median (Modeled) | 90th Percentile (Monitored) | 90th Percentile (Modeled) |
|------------------|---------------|-------------|-------------|-----------------------------|---------------------------|---------------------|-------------------|--------------------|------------------|-----------------------------|---------------------------|
| Daytime Hours | Summer | East | 17 | 0.00 | 22.93 | 25.82 | 27.15 | 27.21 | 26.23 | 42.97 | 32.35 |
| Evening Peak | Summer | East | 89 | 0.00 | 24.94 | 20.11 | 49.58 | 21.89 | 31.85 | 31.24 | 120.50 |
| Morning Peak | Summer | East | 14 | 2.33 | 12.82 | 13.05 | 25.18 | 8.28 | 14.67 | 28.13 | 53.84 |
| Nighttime Hours | Summer | East | 137 | 5.98 | 40.82 | 17.56 | 49.03 | 14.32 | 48.95 | 35.22 | 53.49 |
| All Hours | Summer | East | 257 | 3.12 | 24.64 | 18.74 | 46.47 | 18.51 | 48.56 | 32.69 | 64.51 |
| Daytime Hours | Summer | West | 18 | 9.07 | 67.28 | 79.80 | 77.48 | 83.38 | 77.27 | 109.60 | 89.24 |
| Evening Peak | Summer | West | 103 | 11.91 | 66.15 | 50.43 | 109.21 | 55.46 | 81.71 | 80.12 | 220.36 |
| Morning Peak | Summer | West | 17 | 6.29 | 41.29 | 49.09 | 62.69 | 25.76 | 45.63 | 126.90 | 108.54 |
| Nighttime Hours | Summer | West | 141 | 12.27 | 76.90 | 43.03 | 95.30 | 40.25 | 95.16 | 78.84 | 106.86 |
| All Hours | Summer | West | 279 | 11.87 | 63.84 | 48.51 | 97.30 | 45.92 | 94.26 | 83.56 | 132.29 |

Table 11. Statistical Comparison of Best Model-Predicted CO Concentration at Receptors Parallel to the Roadway and Monitored CO Concentrations (PPB)

| Period | Season | Site | Sample Size | Average Bias | Average Absolute Bias | Std Deviation of Bias | Fractional Bias |
|------------------|---------------|-------------|-------------|----------------|-----------------------|-----------------------|-----------------|
| Daytime Hours - | Winter | East | 22 | -159.31 | 165.85 | 137.10 | -1.41 |
| Evening Peak | Winter | East | 78 | -82.29 | 150.35 | 164.56 | -0.44 |
| Morning Peak | Winter | East | 22 | -270.63 | 270.63 | 231.21 | -1.16 |
| Nighttime Hours | Winter | East | 100 | -238.85 | 244.09 | 230.26 | -1.26 |
| All Hours | Winter | East | 222 | -179.11 | 206.03 | 214.12 | -0.96 |
| Daytime Hours | Winter | West | 30 | -142.59 | 150.20 | 133.99 | -0.81 |
| Evening Peak | Winter | West | 80 | -35.01 | 170.11 | 199.48 | -0.10 |
| Morning Peak | Winter | West | 24 | -177.83 | 281.99 | 310.93 | -0.55 |
| Nighttime Hours | Winter | West | 102 | -194.97 | 213.87 | 223.38 | -0.77 |
| All Hours | Winter | West | 236 | -132.35 | 197.87 | 227.27 | -0.47 |
| Daytime Hours | Summer | East | 17 | -46.82 | 54.07 | 47.07 | -0.86 |
| Evening Peak | Summer | East | 89 | 16.73 | 65.08 | 84.42 | 0.21 |
| Morning Peak | Summer | East | 14 | -5.19 | 33.26 | 42.49 | -0.10 |
| Nighttime Hours | Summer | East | 137 | 9.19 | 38.64 | 47.72 | 0.13 |
| All Hours | Summer | East | 257 | 7.31 | 48.53 | 64.23 | 0.10 |
| Daytime Hours (| Summer | West | 18 | -114.92 | 132.78 | 86.54 | -0.80 |
| Evening Peak | Summer | West | 103 | 23.41 | 141.72 | 172.24 | 0.12 |
| Morning Peak | Summer | West | 17 | 13.47 | 91.40 | 105.47 | 0.11 |
| Nighttime Hours | Summer | West | 141 | 36.56 | 77.95 | 86.78 | 0.26 |
| All Hours | Summer | West | 279 | 20.52 | 105.85 | 130.77 | 0.13 |

Table 12. Statistical Comparison of Best Model-Predicted NO_x Concentration at Receptors Parallel to the Roadway and Monitored NO_x Concentrations (PPB)

| Period | Season | Site | Sample Size | Average Bias | Average Absolute Bias | Std Deviation of Bias | Fractional Bias |
|------------------|---------------|-------------|-------------|--------------|-----------------------|-----------------------|-----------------|
| Daytime Hours - | Winter | East | 22 | -1.92 | 14.68 | 17.19 | -0.07 |
| Evening Peak | Winter | East | 78 | 28.22 | 38.63 | 42.45 | 0.51 |
| Morning Peak | Winter | East | 22 | -19.50 | 33.76 | 41.64 | -0.40 |
| Nighttime Hours | Winter | East | 100 | -14.54 | 28.41 | 39.82 | -0.30 |
| All Hours | Winter | East | 222 | 1.25 | 31.17 | 44.10 | 0.03 |
| Daytime Hours | Winter | West | 30 | 4.17 | 48.58 | 57.99 | 0.05 |
| Evening Peak | Winter | West | 80 | 61.50 | 74.52 | 79.17 | 0.53 |
| Morning Peak | Winter | West | 24 | -27.34 | 69.20 | 85.06 | -0.27 |
| Nighttime Hours | Winter | West | 102 | -2.96 | 40.75 | 52.77 | -0.04 |
| All Hours | Winter | West | 236 | 17.32 | 56.08 | 74.13 | 0.18 |
| Daytime Hours | Summer | East | 17 | 1.34 | 9.67 | 13.97 | 0.05 |
| Evening Peak | Summer | East | 89 | 29.47 | 29.98 | 37.00 | 0.85 |
| Morning Peak | Summer | East | 14 | 12.13 | 17.63 | 21.01 | 0.63 |
| Nighttime Hours | Summer | East | 137 | 31.47 | 31.95 | 14.78 | 0.95 |
| All Hours | Summer | East | 257 | 27.73 | 29.01 | 26.25 | 0.85 |
| Daytime Hours (| Summer | West | 18 | -2.31 | 23.96 | 33.22 | -0.03 |
| Evening Peak | Summer | West | 103 | 58.77 | 59.58 | 64.57 | 0.74 |
| Morning Peak | Summer | West | 17 | 13.61 | 48.98 | 58.58 | 0.24 |
| Nighttime Hours | Summer | West | 141 | 52.27 | 54.42 | 34.07 | 0.76 |
| All Hours | Summer | West | 279 | 48.79 | 54.03 | 51.64 | 0.67 |

Table 13. Distribution of the Ratio of Best Model-Predicted CO Concentration at Receptors Parallel to the Roadway and Monitored CO Concentrations

| Period | Season | Site | Sample Size | Mean Ratio | Median Ratio | 75th Percentile Ratio | 90th Percentile Ratio | 95th Percentile Ratio |
|------------------|---------------|-------------|-------------|-------------|--------------|-----------------------|-----------------------|-----------------------|
| Daytime Hours | Winter | East | 22 | 0.69 | 0.13 | 0.77 | 1.57 | 2.87 |
| Evening Peak | Winter | East | 78 | 2.39 | 0.65 | 1.27 | 2.80 | 7.18 |
| Morning Peak | Winter | East | 22 | 0.35 | 0.26 | 0.57 | 0.70 | 0.79 |
| Nighttime Hours | Winter | East | 100 | 0.62 | 0.26 | 0.47 | 0.89 | 1.72 |
| All Hours | Winter | East | 222 | 1.22 | 0.31 | 0.81 | 1.57 | 2.80 |
| Daytime Hours | Winter | West | 30 | 0.60 | 0.39 | 0.89 | 1.05 | 1.51 |
| Evening Peak | Winter | West | 80 | 0.95 | 0.87 | 1.34 | 1.90 | 2.12 |
| Morning Peak | Winter | West | 24 | 1.64 | 0.47 | 1.05 | 3.14 | 10.31 |
| Nighttime Hours | Winter | West | 102 | 1.37 | 0.48 | 0.91 | 1.42 | 1.81 |
| All Hours | Winter | West | 236 | 1.16 | 0.52 | 1.01 | 1.67 | 2.17 |
| Daytime Hours | Summer | East | 17 | 1.24 | 0.41 | 0.65 | 4.46 | 10.11 |
| Evening Peak | Summer | East | 89 | 2.44 | 0.83 | 2.84 | 6.17 | 8.54 |
| Morning Peak | Summer | East | 14 | 1.33 | 0.97 | 2.33 | 2.70 | 3.03 |
| Nighttime Hours | Summer | East | 137 | 3.19 | 1.24 | 2.46 | 5.38 | 11.12 |
| All Hours | Summer | East | 257 | 2.69 | 1.08 | 2.42 | 5.36 | 8.86 |
| Daytime Hours | Summer | West | 18 | 0.96 | 0.39 | 0.48 | 2.59 | 7.40 |
| Evening Peak | Summer | West | 103 | 2.85 | 0.82 | 2.44 | 5.58 | 9.70 |
| Morning Peak | Summer | West | 17 | 4.27 | 2.03 | 2.89 | 4.82 | 41.31 |
| Nighttime Hours | Summer | West | 141 | 3.53 | 1.47 | 2.88 | 6.07 | 12.03 |
| All Hours | Summer | West | 279 | 3.15 | 1.19 | 2.59 | 5.77 | 10.22 |

Table 14. Distribution of The ratio of Best Model-Predicted NO_x Concentration at Receptors Parallel to the Roadway and Monitored NO_x Concentrations

| Period | Season | Site | Sample Size | Mean Ratio | Median Ratio | 75th Percentile Ratio | 90th Percentile Ratio | 95th Percentile Ratio |
|------------------|---------------|-------------|-------------|-------------|--------------|-----------------------|-----------------------|-----------------------|
| Daytime Hours | Winter | East | 22 | 1.73 | 0.84 | 2.66 | 4.02 | 4.55 |
| Evening Peak | Winter | East | 78 | 2.17 | 1.63 | 2.69 | 4.51 | 7.70 |
| Morning Peak | Winter | East | 22 | 1.07 | 0.56 | 1.10 | 2.46 | 3.17 |
| Nighttime Hours | Winter | East | 100 | 1.20 | 0.80 | 1.45 | 2.25 | 3.56 |
| All Hours | Winter | East | 222 | 1.58 | 0.94 | 2.06 | 3.37 | 4.57 |
| Daytime Hours | Winter | West | 30 | 2.90 | 1.29 | 2.72 | 6.79 | 8.19 |
| Evening Peak | Winter | West | 80 | 2.10 | 1.62 | 2.54 | 4.95 | 5.76 |
| Morning Peak | Winter | West | 24 | 1.61 | 0.82 | 1.53 | 5.28 | 5.92 |
| Nighttime Hours | Winter | West | 102 | 1.51 | 1.04 | 1.84 | 2.57 | 3.93 |
| All Hours | Winter | West | 236 | 1.90 | 1.14 | 2.27 | 3.83 | 5.86 |
| Daytime Hours | Summer | East | 17 | 6.57 | 1.01 | 1.18 | 12.97 | 82.92 |
| Evening Peak | Summer | East | 89 | 4.12 | 1.56 | 4.66 | 10.11 | 15.61 |
| Morning Peak | Summer | East | 14 | 4.14 | 2.67 | 4.27 | 8.13 | 21.93 |
| Nighttime Hours | Summer | East | 137 | 7.07 | 3.43 | 6.11 | 11.20 | 29.04 |
| All Hours | Summer | East | 257 | 5.86 | 2.66 | 4.88 | 10.94 | 19.13 |
| Daytime Hours | Summer | West | 18 | 1.82 | 0.91 | 1.02 | 7.45 | 9.54 |
| Evening Peak | Summer | West | 103 | 3.50 | 1.63 | 3.92 | 9.79 | 10.82 |
| Morning Peak | Summer | West | 17 | 6.54 | 2.07 | 4.11 | 15.34 | 60.36 |
| Nighttime Hours | Summer | West | 141 | 4.10 | 2.47 | 5.12 | 8.26 | 12.51 |
| All Hours | Summer | West | 279 | 3.88 | 2.09 | 4.19 | 8.56 | 12.27 |

Figure 13. Scatter Plots of Dilution Ratios Calculated from Model Predictions and Monitored Concentrations

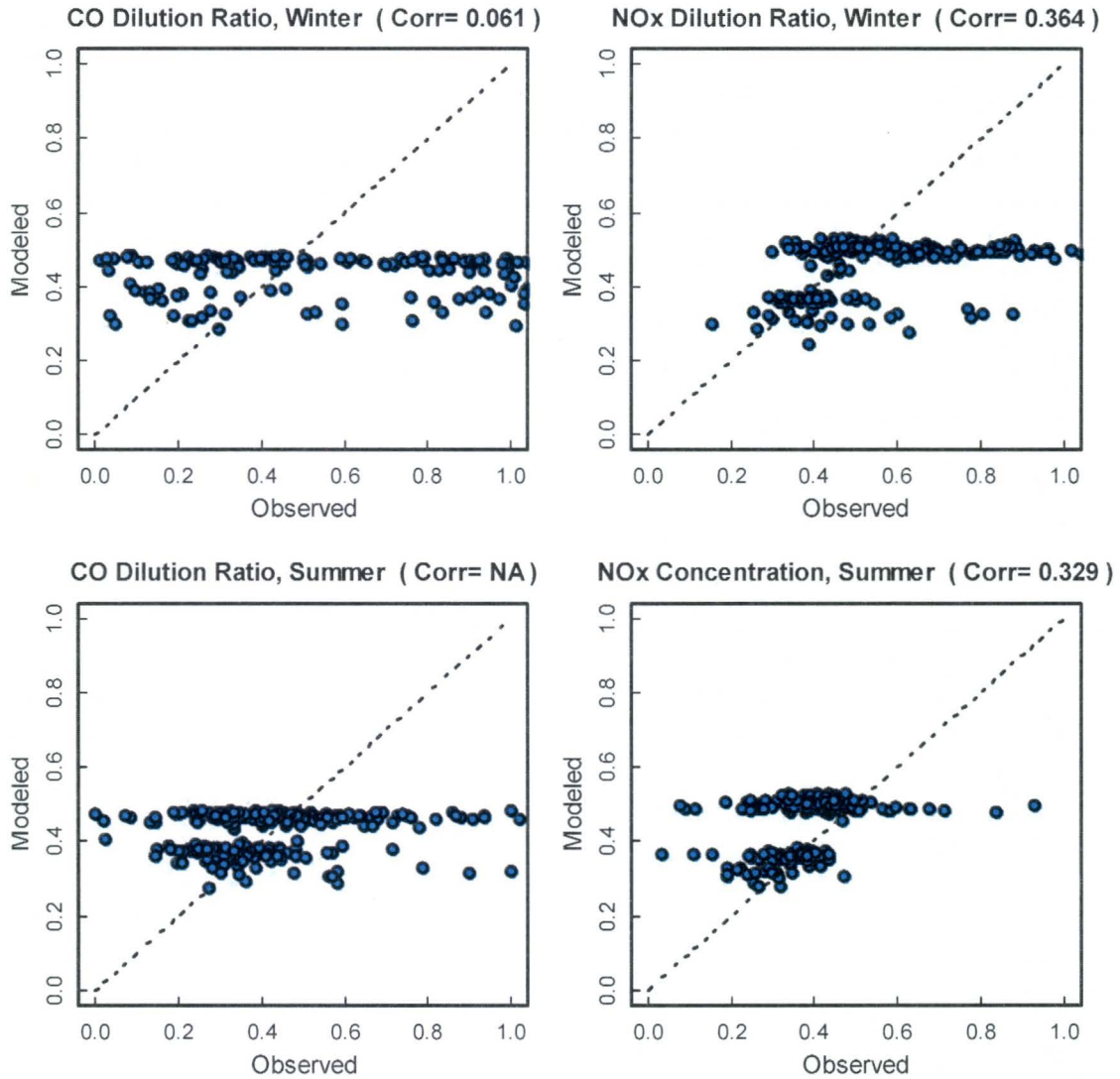


Figure 14. Scatter Plots of Dilution Ratios Calculated from Model-Predicted and Monitored CO Concentration Data for Four Intra-Day Periods during Summer

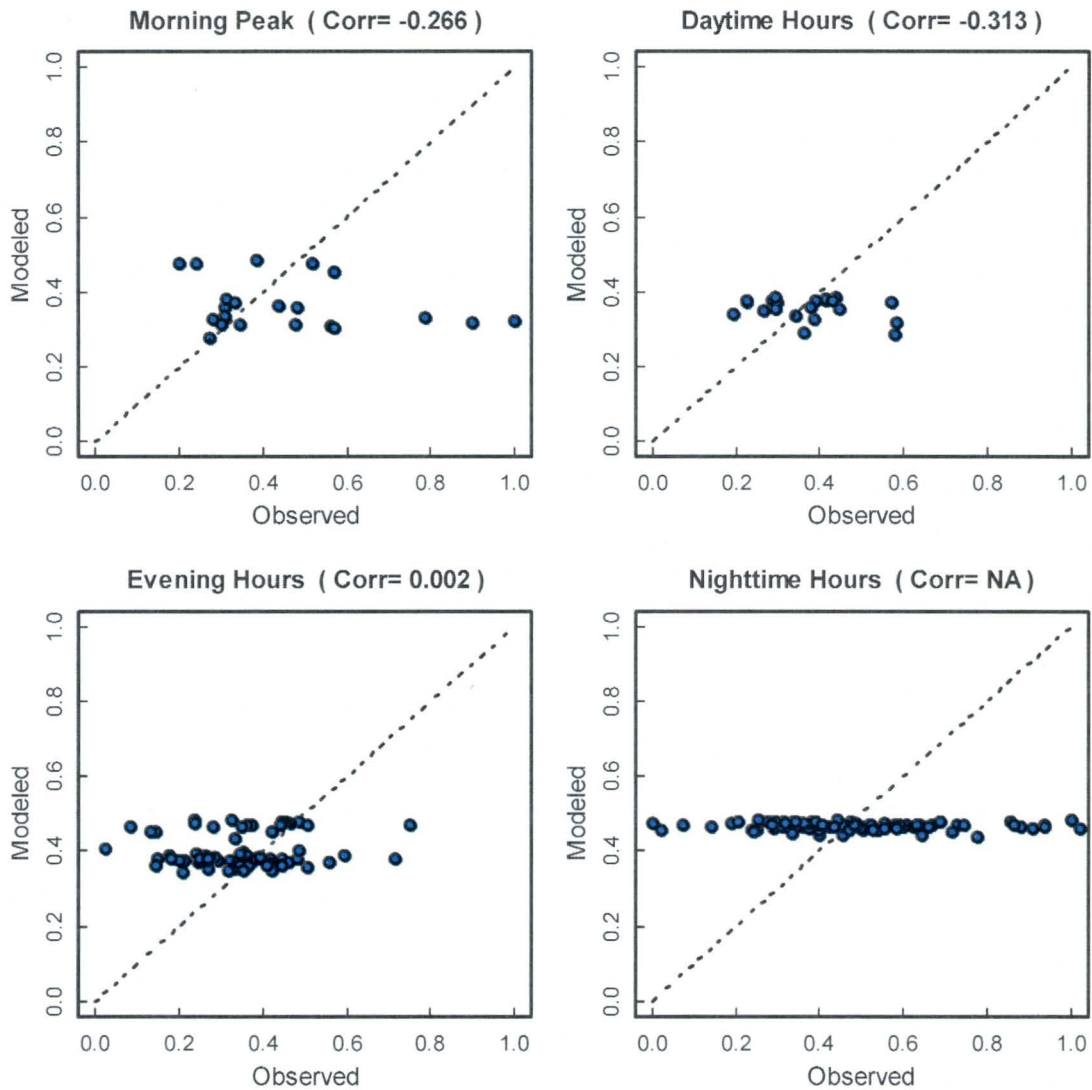


Figure 15. Scatter Plots of Dilution Ratios Calculated from Model-Predicted and Monitored NO_x Concentration Data for Four intra-Day Periods during Summer

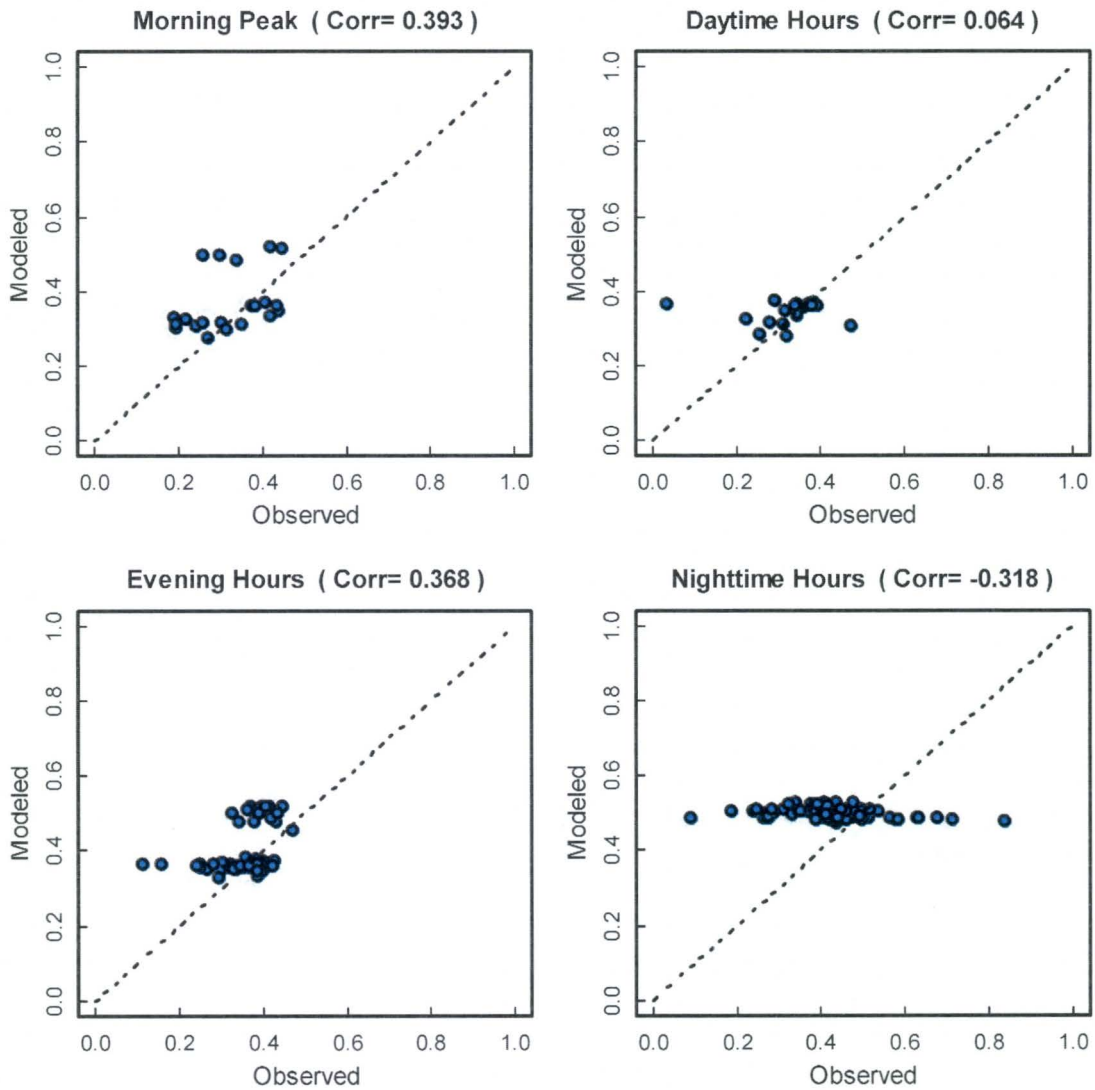


Figure 16. Scatter Plots of Dilution Ratios Calculated from Model-Predicted and Monitored CO Concentration Data for Four Intra-Day Periods during Winter

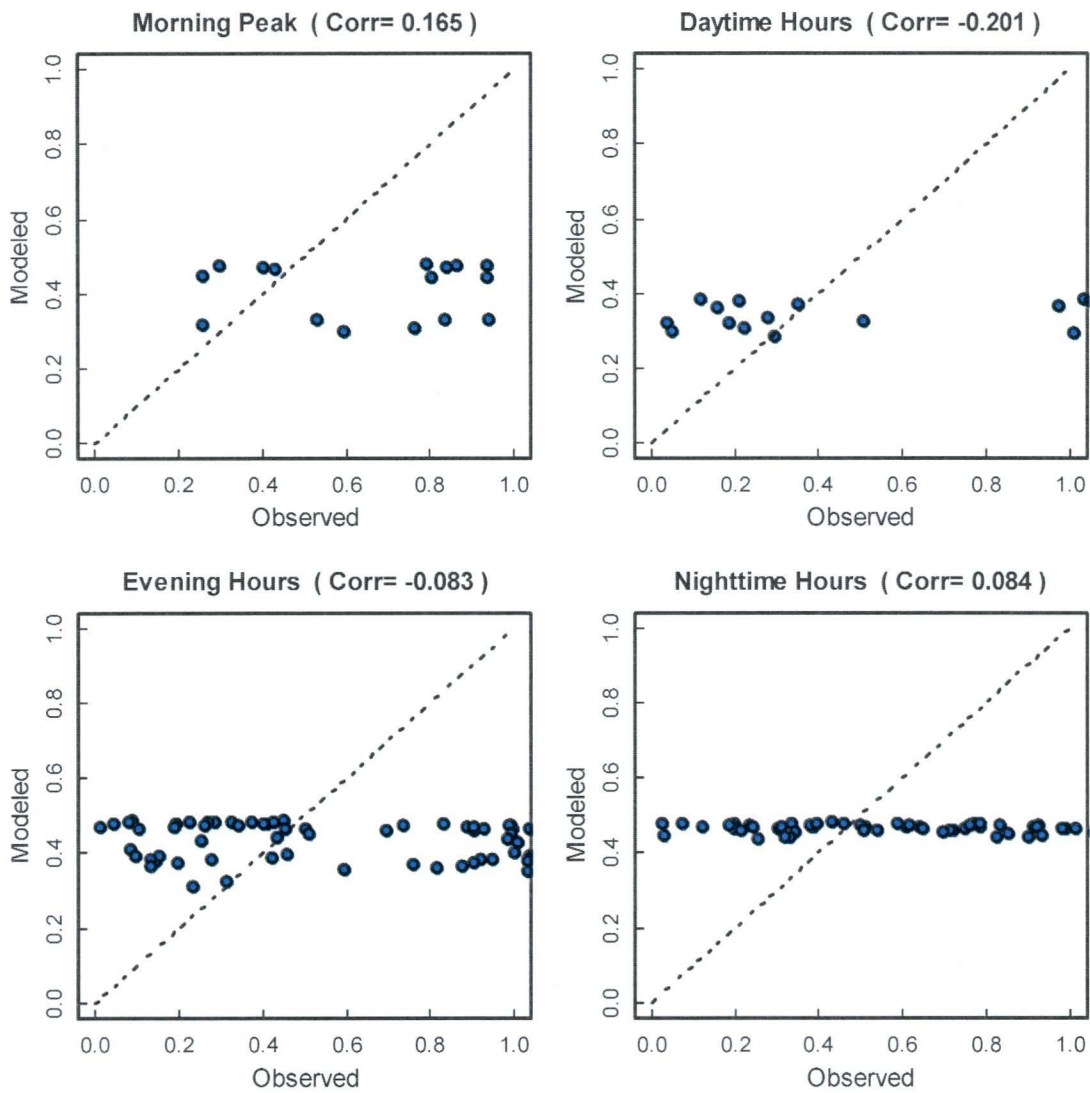


Figure 17. Scatter Plots of Dilution Ratios Calculated from Model-Predicted and Monitored NO_x Concentration Data for Four Intra-Day Periods during Winter

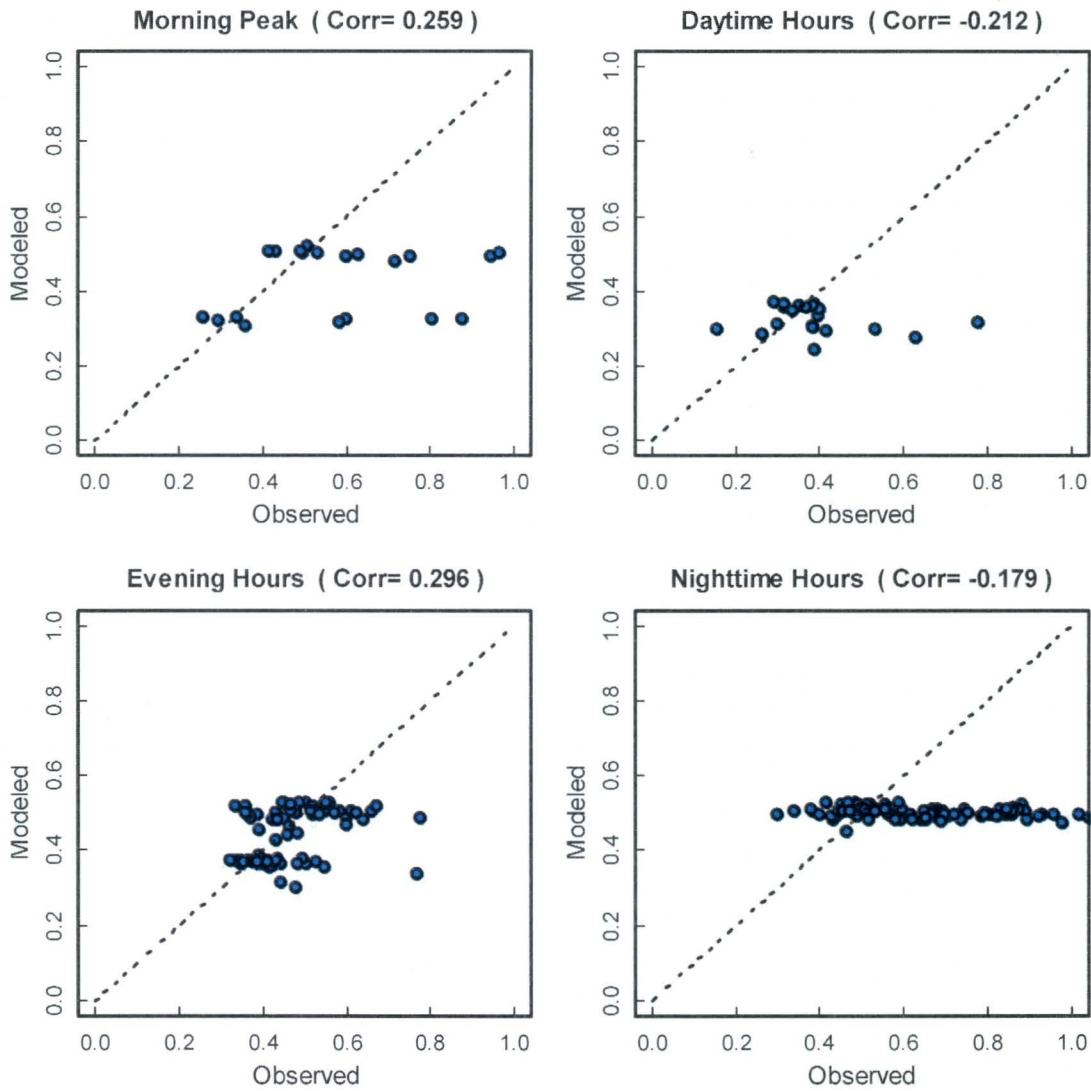


Table 15. Comparison of the Average, Median, 75th and 90th Percentile of Modeled and Monitored Dilution Ratios of CO Concentrations

| Period | Season | Sample Size | Mean Dilution (Modeled) | Mean Dilution (Monitored) | Median Dilution (Modeled) | Median Dilution (Monitored) | 75 th Percentile (Modeled) | 75 th Percentile (Monitored) | 90 th Percentile (Modeled) | 90 th Percentile (Monitored) |
|------------------|---------------|-------------|-------------------------|---------------------------|---------------------------|-----------------------------|---------------------------------------|---|---------------------------------------|---|
| Daytime Hours | Winter | 21 | 0.341 | 0.731 | 0.336 | 0.508 | 0.380 | 1.056 | 0.386 | 1.267 |
| Evening Peak | Winter | 77 | 0.432 | 0.657 | 0.459 | 0.758 | 0.476 | 1.030 | 0.482 | 1.080 |
| Morning Peak | Winter | 21 | 0.408 | 1.511 | 0.445 | 0.834 | 0.471 | 0.940 | 0.476 | 2.245 |
| Nighttime Hours | Winter | 100 | 0.466 | 1.869 | 0.468 | 0.957 | 0.475 | 1.365 | 0.479 | 2.059 |
| All Hours | Winter | 219 | 0.437 | 1.299 | 0.463 | 0.862 | 0.473 | 1.121 | 0.480 | 1.651 |
| Daytime Hours | Summer | 17 | 0.349 | 0.367 | 0.356 | 0.363 | 0.374 | 0.413 | 0.378 | 0.581 |
| Evening Peak | Summer | 89 | 0.398 | 0.360 | 0.380 | 0.353 | 0.432 | 0.432 | 0.472 | 0.504 |
| Morning Peak | Summer | 14 | 0.357 | 0.548 | 0.319 | 0.521 | 0.453 | 0.788 | 0.474 | 1.000 |
| Nighttime Hours | Summer | 133 | 0.466 | 0.695 | 0.466 | 0.484 | 0.475 | 0.667 | 0.478 | 1.021 |
| All Hours | Summer | 253 | 0.428 | 0.546 | 0.458 | 0.413 | 0.469 | 0.556 | 0.477 | 0.821 |

Table 16. Comparison of the Average, Median, 75th and 90th Percentile of Modeled and Monitored Dilution Ratios of NO_x Concentrations

| Period | Season | Sample Size | Mean Dilution (Modeled) | Mean Dilution (Monitored) | Median Dilution (Modeled) | Median Dilution (Monitored) | 75 th Percentile (Modeled) | 75 th Percentile (Monitored) | 90 th Percentile (Modeled) | 90 th Percentile (Monitored) |
|------------------|---------------|-------------|-------------------------|---------------------------|---------------------------|-----------------------------|---------------------------------------|---|---------------------------------------|---|
| Daytime Hours | Winter | 21 | 0.329 | 0.387 | 0.334 | 0.382 | 0.363 | 0.395 | 0.367 | 0.530 |
| Evening Peak | Winter | 77 | 0.446 | 0.464 | 0.484 | 0.445 | 0.506 | 0.517 | 0.523 | 0.599 |
| Morning Peak | Winter | 21 | 0.434 | 0.630 | 0.493 | 0.582 | 0.504 | 0.749 | 0.509 | 0.942 |
| Nighttime Hours | Winter | 100 | 0.501 | 0.651 | 0.501 | 0.618 | 0.509 | 0.785 | 0.519 | 0.892 |
| All Hours | Winter | 219 | 0.458 | 0.558 | 0.495 | 0.513 | 0.507 | 0.653 | 0.520 | 0.843 |
| Daytime Hours | Summer | 17 | 0.342 | 0.313 | 0.351 | 0.339 | 0.367 | 0.343 | 0.371 | 0.382 |
| Evening Peak | Summer | 89 | 0.399 | 0.367 | 0.366 | 0.379 | 0.457 | 0.401 | 0.517 | 0.419 |
| Morning Peak | Summer | 14 | 0.364 | 0.256 | 0.316 | 0.256 | 0.486 | 0.300 | 0.497 | 0.336 |
| Nighttime Hours | Summer | 133 | 0.502 | 0.411 | 0.504 | 0.411 | 0.509 | 0.457 | 0.523 | 0.507 |
| All Hours | Summer | 253 | 0.447 | 0.380 | 0.489 | 0.384 | 0.505 | 0.426 | 0.519 | 0.474 |

Table 17. Distribution of the Ratio of Modeled CO Dilution Ratio to Monitored CO Dilution Ratio

| Period | Season | Sample Size | Mean | Median | 75 th Percentile | 90 th Percentile | 95 th Percentile |
|------------------|---------------|-------------|--------------|--------------|-----------------------------|-----------------------------|-----------------------------|
| Daytime Hours | Winter | 21 | 1.561 | 0.642 | 1.733 | 3.270 | 6.391 |
| Evening Peak | Winter | 77 | 1.837 | 0.578 | 1.476 | 2.905 | 5.520 |
| Morning Peak | Winter | 21 | 0.628 | 0.509 | 0.631 | 1.238 | 1.594 |
| Nighttime Hours | Winter | 100 | 1.095 | 0.475 | 0.938 | 1.831 | 2.497 |
| All Hours | Winter | 219 | 1.356 | 0.513 | 1.222 | 2.433 | 4.523 |
| Daytime Hours | Summer | 17 | 1.067 | 0.958 | 1.318 | 1.683 | 1.763 |
| Evening Peak | Summer | 89 | 1.482 | 1.092 | 1.409 | 2.063 | 2.556 |
| Morning Peak | Summer | 14 | 0.893 | 0.724 | 1.042 | 1.968 | 2.372 |
| Nighttime Hours | Summer | 133 | 1.221 | 0.966 | 1.276 | 1.635 | 1.921 |
| All Hours | Summer | 253 | 1.285 | 1.012 | 1.318 | 1.805 | 2.318 |

Table 18. Distribution of the Ratio of Modeled NO_x Dilution Ratio to Monitored NO_x Dilution Ratio

| Period | Season | Sample Size | Mean | Median | 75 th Percentile | 90 th Percentile | 95 th Percentile |
|------------------|---------------|-------------|--------------|--------------|-----------------------------|-----------------------------|-----------------------------|
| Daytime Hours | Winter | 21 | 0.940 | 0.953 | 1.043 | 1.166 | 1.276 |
| Evening Peak | Winter | 77 | 0.991 | 0.966 | 1.088 | 1.300 | 1.414 |
| Morning Peak | Winter | 21 | 0.804 | 0.825 | 1.037 | 1.187 | 1.233 |
| Nighttime Hours | Winter | 100 | 0.834 | 0.790 | 1.007 | 1.130 | 1.259 |
| All Hours | Winter | 219 | 0.896 | 0.892 | 1.051 | 1.180 | 1.322 |
| Daytime Hours | Summer | 17 | 1.615 | 1.063 | 1.134 | 1.481 | 10.560 |
| Evening Peak | Summer | 89 | 1.125 | 1.026 | 1.248 | 1.407 | 1.489 |
| Morning Peak | Summer | 14 | 1.483 | 1.480 | 1.682 | 1.942 | 2.716 |
| Nighttime Hours | Summer | 133 | 1.364 | 1.229 | 1.432 | 1.773 | 1.964 |
| All Hours | Summer | 253 | 1.303 | 1.165 | 1.345 | 1.633 | 1.925 |

Table 19. Comparison of Monitored and Modeled CO Concentrations (ppb) for Locations with and without the Sound Wall Using Ning et al. (2010) Data

| Hour | Monitored Mean CO (ppb) | Modeled Mean CO (ppb) |
|----------------|-------------------------|-----------------------|
| Wall | | |
| 14:00 | 488.235 (17) | 166.081 (45) |
| 15:00 | 496.078 (51) | 164.857 (50) |
| 16:00 | 385.393 (89) | 258.335 (57) |
| 17:00 | 359.155 (71) | 297.838 (56) |
| 18:00 | 233.333 (27) | 336.785 (57) |
| No Wall | | |
| 14:00 | 0 (0) | 185.419 (45) |
| 15:00 | 747.826 (46) | 182.97 (50) |
| 16:00 | 572.093 (86) | 269.254 (57) |
| 17:00 | 448.305 (118) | 306.404 (56) |
| 18:00 | 343.21 (81) | 346.991 (57) |

Notes: The comparison is done using the average concentrations at afternoon hours for monitored and modeled concentrations in the months of June and July of 2009. The values in parenthesis indicate the number of observations.

Figure 18. Temporal Profiles of Light-Duty (Passenger 2/3-Axle Trucks) and Heavy-Duty (4 or More Axle Vehicles) Traffic on the I-710 from Historical (15 May–15 September 2002) Caltrans Weigh-In Motion Sensors.

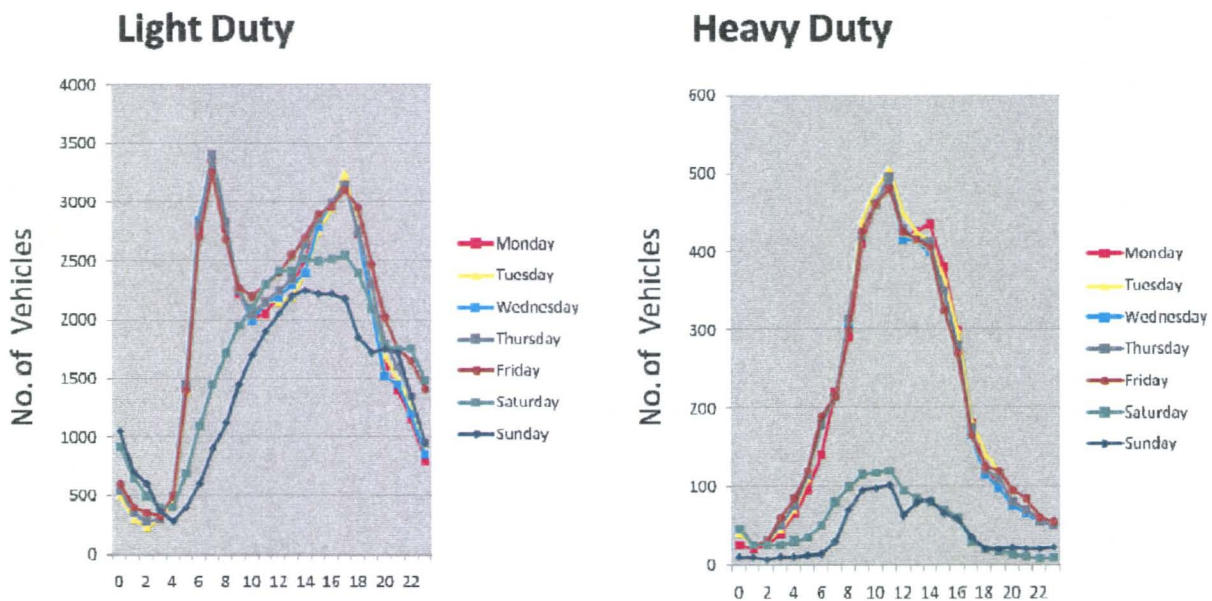


Figure 19. Scatter Plots of Observed and Modeled NO_x Concentrations at the East Monitor Using the Temporal Profile Used in I-710 EIR/EIS (Dots in Blue, Left Panels) and the Profile from Caltrans I-710 Weigh in Motion Traffic Volume Data (Dots in Red, Right Panels) for All Hours. (Pearson Correlation Coefficients are Included in the Parenthesis.)

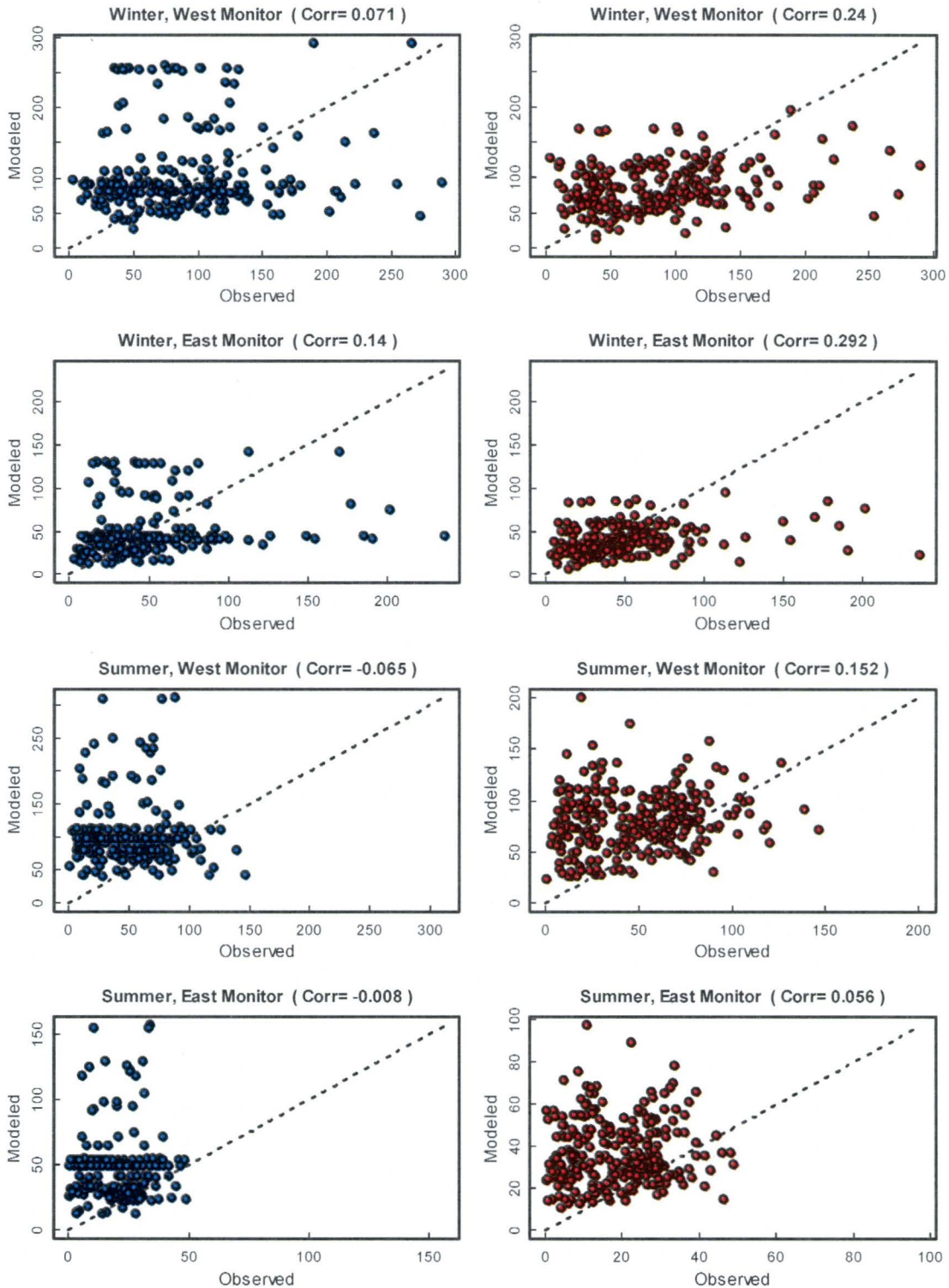
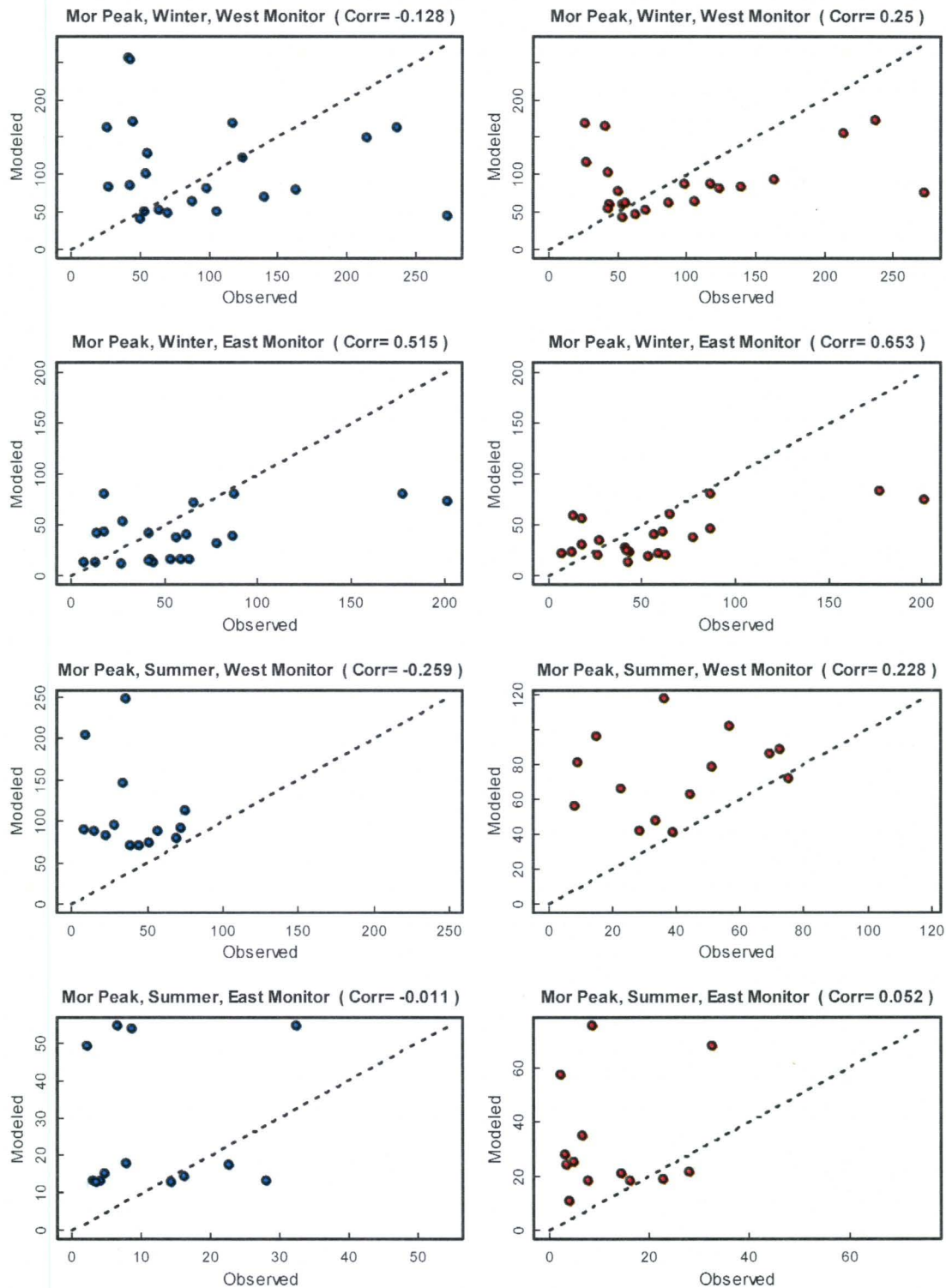


Figure 20. Scatter Plots of Observed and Modeled NO_x Concentrations at the East Monitor Using the Temporal Profile Used in I-710 EIR/EIS (Dots in Blue, Left Panels) and the Profile from Caltrans I-710 Weigh In Motion Traffic Volume Data (Dots in Red, Right Panels) for the Morning Peak Hours. (Pearson Correlation Coefficients Are Included in the Parenthesis.)



**Figure 21. Scatter Plots of Observed and Modeled NO_x Concentrations at the East Monitor Using the Temporal Profile Used in I-710 EIR/EIS (Dots in Blue, Left Panels) and the Profile from Caltrans I-710 Weigh In Motion Traffic Volume Data (Dots in Red, Right Panels) for the Daytime Hours.
(Pearson Correlation Coefficients Are Included in the Parenthesis.)**

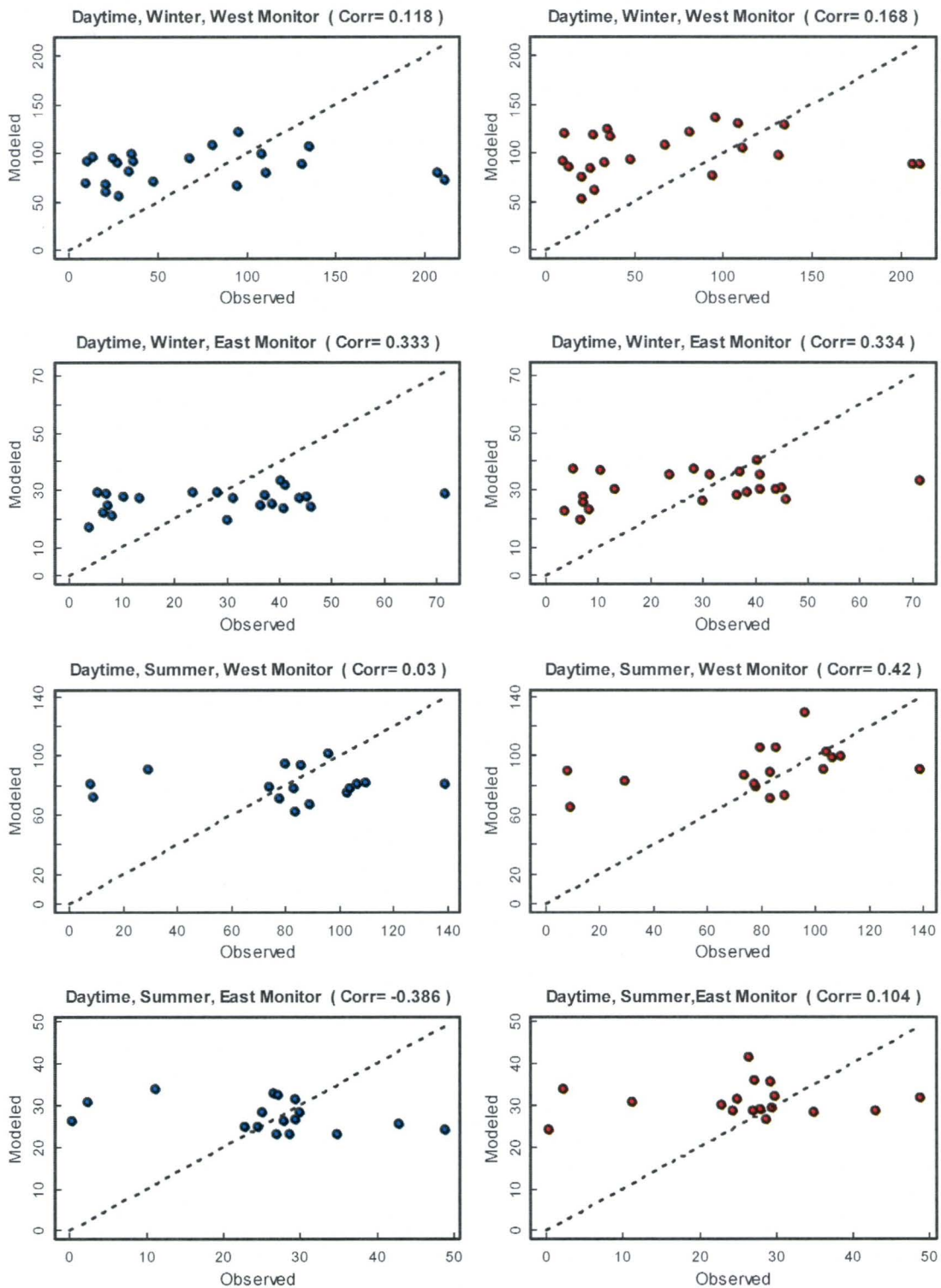


Figure 22. Scatter Plots of Observed and Modeled NO_x Concentrations at the East Monitor Using the Temporal Profile Used in I-710 EIR/EIS (Dots in Blue, Left Panels) and the Profile from Caltrans I-710 Weigh In Motion Traffic Volume Data (Dots in Red, Right Panels) for the Evening Peak. (Pearson Correlation Coefficients Are Included in the Parenthesis.)

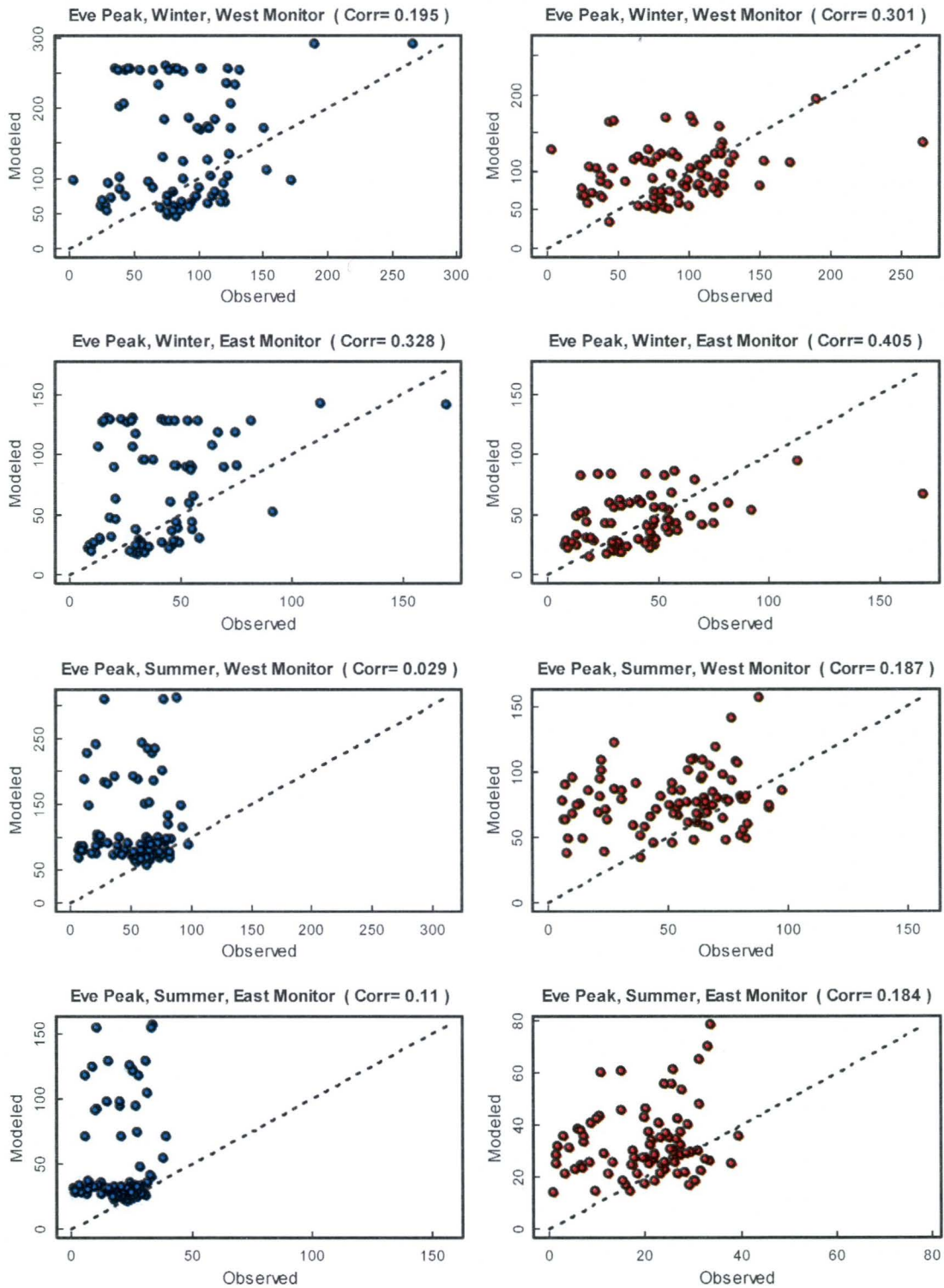
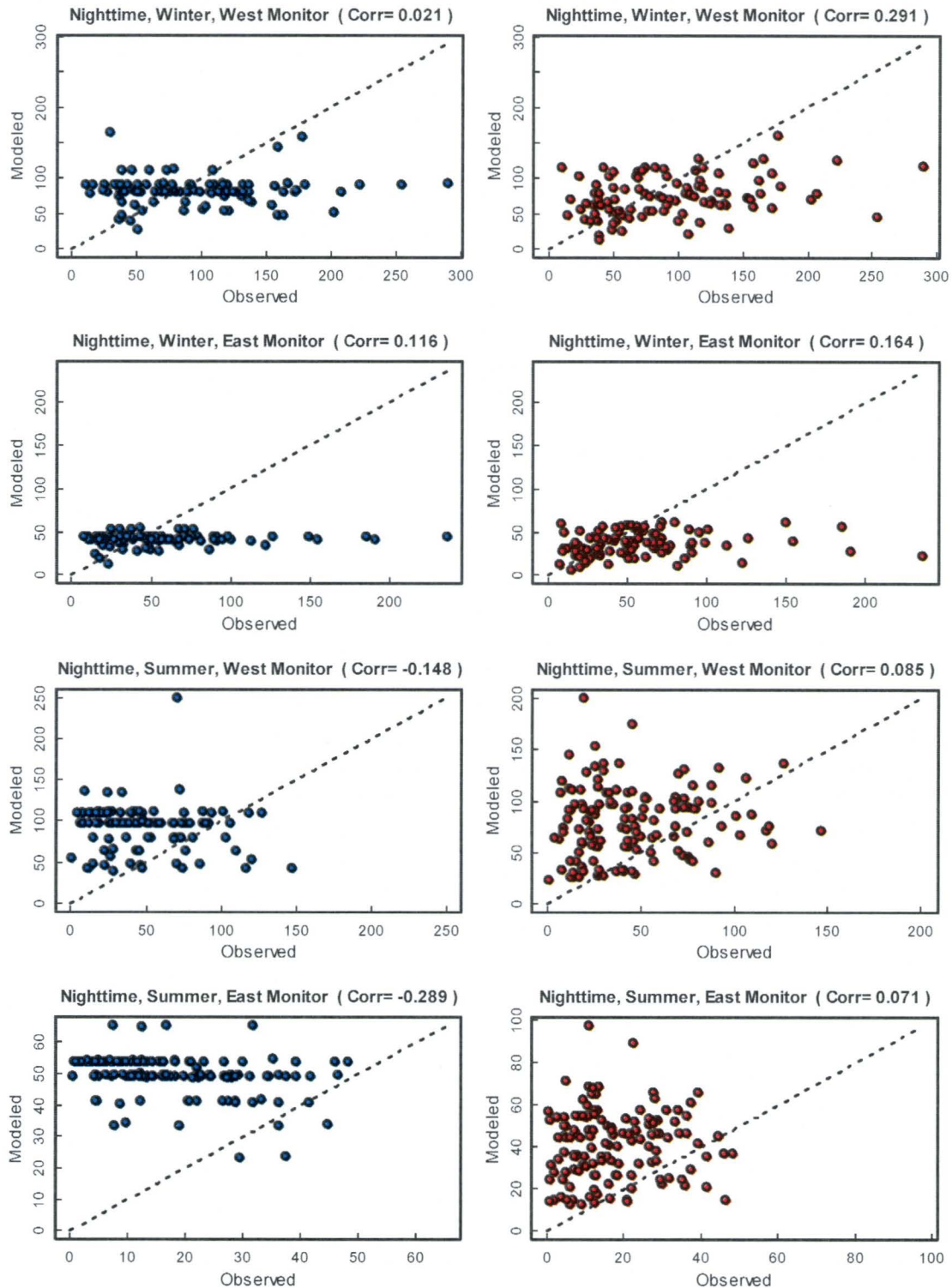


Figure 23. Scatter Plots of Observed and Modeled NO_x Concentrations at the East Monitor Using the Temporal Profile Used in I-710 EIR/EIS (Dots in Blue, Left Panels) and the Profile from Caltrans I-710 Weigh In Motion Traffic Volume Data (Dots in Red, Right Panels) for the Nighttime Hours. (Pearson Correlation Coefficients Are Included in the Parenthesis.)



6. References

- Arhami, M., M. Sillanpaa, et al. (2009). "Size-segregated inorganic and organic components of PM in the communities of the Los Angeles harbor." Aerosol Science and Technology 43(2): 145-160.
- Karner, A. A., D. S. Eisinger, et al. (2010). "Near-Roadway Air Quality: Synthesizing the Findings from Real-World Data." Environmental science & technology.
- Kozawa, K. H., S. A. Fruin, et al. (2009). "Near-road air pollution impacts of goods movement in communities adjacent to the Ports of Los Angeles and Long Beach." Atmospheric Environment 43(18): 2960-2970.
- Moore, K., M. Krudysz, et al. (2009). "Intra-community variability in total particle number concentrations in the San Pedro Harbor area (Los Angeles, California)." Aerosol Science and Technology 43(6): 587-603.
- Ning, Z., N. Hudda, et al. (2010). "Impact of roadside noise barriers on particle size distributions and pollutants concentrations near freeways." Atmospheric Environment 44(26): 3118-3127.
- Zhu, Y., W. C. Hinds, et al. (2002). "Concentration and size distribution of ultrafine particles near a major highway." Journal of the Air & Waste Management Association 52(9): 1032-1042.

Appendix A. Comparative Studies

Following is a comparative summary of some near-roadway studies conducted in the LA area.

| | Arhami et al. (2009) | Kozawa et al. (2009) | Moore et al. (2009) | Ning et al. (2010) |
|------------------------------------|---|--|---|---|
| Main Objective of the Study | Characterize the chemical composition of ultrafine, accumulation mode and coarse particles | Characterize pollutant concentrations in communities adjacent to Ports of Los Angeles and Long Beach | Characterize the intra-community variability in ultrafine particle concentrations. | Characterize the effect of roadside barriers on near-roadway air quality. |
| Sampling Locations | Concurrent sampling at six sites - five sites in the LA port area, one at USC. One of the sites is 1 km downwind from I-710 | Mobile monitoring along two routes. One route included I-710 and surrounding areas | Fourteen monitoring sites in two clusters – San Pedro and West Long Beach clusters. Two sites in the vicinity of I-710. | Two sampling sites each for I-405 and I-710, one with and one without sound wall. |
| Sampling Dates | Seven week period between March and May 2007 | Winter and Summer months of 2007 | February 12, 2007 through December 11, 2007 | June–July 2009, afternoon hours |
| Sampling Frequency | Daily, from Monday to Friday. | Twice daily, morning and afternoon | One-minute intervals | PM at 5 min intervals, CO and NO ₂ at 1 minute intervals |
| Sampled Pollutants | Size-segregated PM and meteorological data | Particle size distribution of mass, particle count, CO, NO ₂ , NO _x , NO, and VOCs | Total particle number concentrations and meteorological data | Particle size distribution, CO, NO ₂ , and meteorological data |

| | Arhami et al. (2009) | Kozawa et al. (2009) | Moore et al. (2009) | Ning et al. (2010) |
|---------------------|---|--|--|--|
| Key Findings | The particulate organic matter dominated chemical composition in quasi-ultrafine particle size range, followed by sulfate and elemental carbon. Strong chemical signatures of vehicle and marine emissions. | Pollutants with large diesel-vehicle contribution, such as black carbon, nitric oxide, ultrafine particles and PAH are elevated by two to five times within 150m of freeways and two to three times 150 m downwind of arterial roads with significant amount of diesel traffic | Significant intra-community variability was observed in the San Pedro area. The ultrafine particle concentrations at sites within a few km of each other can vary by a factor of up to 10. | A “concentration deficit” zone is formed near the sound wall, however, pollutant concentration surge further downwind at 80 – 100m away from freeway. The particle concentrations reach background levels at farther distances of 250–400m for stretches along the sound wall as compared to 150 –200m at the sites without roadside noise barriers. |